Forest Ecology and Management 497 (2021) 119480

Contents lists available at ScienceDirect

Forest Ecology and Management

journal homepage: www.elsevier.com/locate/foreco

Microclimate and land surface temperature in a biodiversity enriched oil palm plantation

Laura Somenguem Donfack [a,c,*], Alexander Röll [b], Florian Ellsäßer [b], Martin Ehbrecht [a], Bambang Irawan [d], Dirk Hölscher [b,e], Alexander Knohl [e,f], Holger Kreft [c,e], Eduard J. Siahaan [d], Leti Sundawati [g], Christian Stiegler [f], Delphine Clara Zemp [c,e,h]

[a] University of Goettingen, Silviculture and Forest Ecology of the Temperate Zones, Büsgenweg 1, 37077 Göttingen, Germany
[b] University of Goettingen, Tropical Silviculture and Forest Ecology, Büsgenweg 1, 37077 Göttingen, Germany
[c] University of Goettingen, Biodiversity, Macroecology and Biogeography, Büsgenweg 1, 37077 Göttingen, Germany
[d] University of Jambi, Faculty of Forestry, Jln Raya Jambi, 36361 Jambi, Indonesia
[e] University of Goettingen, Centre of Biodiversity and Sustainable Land Use, Büsgenweg 1, 37077 Göttingen, Germany
[f] University of Goettingen, Bioclimatology, Büsgenweg 2, 37077 Göttingen, Germany
[g] Bogor Agricultural University, Department of Forest Management, Kampus IPB Darmaga, 16680 Bogor, Indonesia
[h] University of Neuchâtel, Institute of Biology, Conservation Biology Lab, Rue Emilie-Argand 11, CH-2000 Neuchâtel, Switzerland

ARTICLE INFO

Keywords:
Microclimate
Land surface temperature
iButton
Drone-based thermography
Oil palm
Biodiversity enrichment agroforestry experiment

ABSTRACT

Agroforestry options such as mixed-species tree planting and natural regeneration in oil palm plantations may alleviate negative effects of forest loss on biodiversity and ecosystem functioning. The effects of agroforestry on microclimate and land surface temperatures (LST) remain largely unknown despite their central role in controlling abiotic and biotic factors and in buffering climate at a larger scale. We assessed spatial and temporal microclimate and LST variability in a biodiversity enrichment experiment, in which tree islands have been planted in an oil palm plantation in Sumatra (Indonesia). Four years after establishment of the experiment, we measured microclimate and LST using mini microclimate sensors and drone-recorded thermal images. We examined experimental effects of tree species richness (0, 1, 2, 3 or 6), plot size (25 m^2, 100 m^2, 400 m^2, 1600 m^2) and stand structural complexity on microclimate and LST. Diurnal patterns showed ambient air temperature peaks and relative humidity (RH) minima at 3 pm, whereas diurnal soil temperatures peaked around 6 pm. The lowest LST were observed from oil palm canopy leaves and the highest from bare soils and understorey vegetation (including trees). Spatial and temporal ranges of ambient air temperature were smaller than LST ranges, and average ambient air temperature and LST were positively correlated. Tree species diversity had no overall significant effect neither on microclimate nor LST, but humidity was higher in planted tree islands compared to natural regeneration only. Smaller plots were characterized by higher mean air, soil and LST, compared to larger plots. Structurally complex plots were associated with low mean and maximum values of ambient air temperature, soil temperature and LST and high mean and minimum RH. Still, conditions were hotter and drier in several experimental plots compared to conventional oil palm plantations, considering a higher transpiration in the latest. We conclude that stand structural complexity and tree island size control microclimate and LST in the experimental oil palm agroforests, but alleviating the harsh microclimate conditions in oil palm plantations might take longer to occur.

1. Introduction

Deforestation and forest degradation are often driven by the agricultural land expansion (crops and grazing land), which has become very pronounced over time (Gibbs et al., 2010; IPBS, 2018; Vijay et al., 2016). One of many examples is Indonesia, where the vast expansion of oil palm and other monocultural crops has contributed to deforestation in recent decades (Abood et al., 2015). Oil palm products are now

Abbreviations: LST, Land Surface Temperature; RH, Relative Humidity.

* Corresponding author.
E-mail addresses: laura.ds@uni-goettingen.de, lauradonfack@yahoo.fr (L.S. Donfack).

https://doi.org/10.1016/j.foreco.2021.119480
Received 31 March 2021; Received in revised form 6 June 2021; Accepted 20 June 2021
Available online 9 July 2021

Indonesia's top commodity (FAO, 2017), providing raw and derivative products for local and global markets (Sequiño and Magallon-Avenido, 2015). On the other hand, forest conversion to oil palm plantations results into biodiversity impairment and losses of key ecosystem functions (Clough et al., 2016; Drescher et al., 2016; Hardwick et al., 2015; Meijaard et al., 2020; Qaim et al., 2020; Vijay et al., 2016).

Forest conversion into other land-use systems modifies the vegetation structure and consequently microclimate (Luskin and Potts, 2011; Meijide et al., 2018) and land surface temperatures (LST) (Sabajo et al., 2017). At the land-atmosphere interface, microclimate affects organisms which determine, through various interactions, ecosystem structure, functions and compositions (Zellweger et al., 2020). Agroforests, e.g., in form of oil palm plantations enriched with native tree species, are regarded to be an alternative to monoculture cultivation and can (partially) conserve or restore biodiversity and key ecosystem functions (Koh et al., 2009). However, there remains a need for studies in (oil palm) agroforests to better understand microclimate and its interaction with land use at local scales as the basis for better understanding and predicting microclimate heterogeneity and regulative functions (Potter et al., 2013; Zellweger et al., 2019).

Microclimate and LST interact with key ecological processes (i.e., nutrient cycling) and plant physiology (i.e., growth and transpiration) (Bonan, 2016; Sabajo et al., 2017; Zellweger et al., 2019). It has been suggested that both microclimate and LST affect biotic factors such as the understorey vegetation and other organisms, which in turn could buffer climate warming at a larger scale (De Frenne et al., 2013; Zellweger et al., 2019). Previous research stated that forest conversion into oil palm monocultures leads to higher air temperatures, lower relative humidity and largely increased diurnal amplitudes for both variables in Indonesia (Böhnert et al., 2016; Meijide et al., 2018) and Malaysia (Luskin and Potts, 2011). In tropical rainforests, spatial heterogeneity of LST compared to ambient air temperature was reported to be higher (Scheffers et al., 2017), while the opposite could be expected for monocultures. Only few previous studies have examined the relationship between LST and ambient air temperature; therein, a study in a temperate forest observed a relatively high correlation between the two variables (Kawashima et al., 1999).

Land surface temperatures can be recorded in thermal images from unmanned aerial vehicles (UAV) (Banu et al., 2016; Berni et al., 2009; Faye et al., 2016). Compared to satellite imagery, UAV-based schemes are more flexible in terms of recording time and frequency and can achieve much higher image resolution (Ellsäßer et al., 2021; Laliberte, 2009). Microclimate is classically assessed from stations where at least ambient air temperature and relative humidity are recorded; but smaller and cheaper temperature and humidity sensors become broadly available, which offers chances for microclimatic assessment schemes with simultaneous measurements at multiple vertical and horizontal positions (Hardwick et al., 2015; Hubbart et al., 2005; Shin et al., 2017; Zellweger et al., 2020).

The complexity of vegetation structure (stand structural complexity), i.e., the heterogeneity of biomass distribution in three-dimensional space, has been shown to strongly influence microclimate (Ehbrecht et al., 2019). The structural complexity in oil palm agroforests influences biodiversity and ecosystem functions (Foster et al., 2011; Zellweger et al., 2013) and reciprocally, tree diversity enhances structural complexity in oil palm plantations (Zemp et al., 2019a). Ehbrecht et al. (2017) and Juchheim et al. (2019) observed an increasing stand structural complexity with increasing tree species diversity in temperate forests. Therefore, both stand structural complexity and species diversity are potential determinant of microclimate conditions in monocultures and agroforest stands.

Our study integrated drone-based thermal images and microclimate data measured within a large scale and long term biodiversity enrichment experiment developed by Teuscher et al. (2016) in Sumatra, Indonesia. Here, we (1) studied the temporal change of three microclimate variables (ambient air temperature, relative humidity and soil temperature) within three plots of interest taken as example, to illustrate the general pattern. We (2) assessed the correlation between LST and ambient air temperature under the canopy within experimental plots. We (3) assessed microclimate and LST variability across plot size, species diversity and stand structural complexity indexes (SSCI). We hypothesised that the LST and the mean ambient air temperature under the canopy are positively correlated. Then, we assumed that with increasing plot size and tree species diversity level, lower temperatures and higher humidity conditions would occur. Lastly, we expected that increasing structural complexity favours lower temperatures and higher humid conditions.

2. Methods

2.1. Study region

This study was conducted as part of the collaborative project EFForTS [Ecological and Socioeconomic Functions of Tropical Lowland Rainforest Transformation Systems] (Drescher et al., 2016) in the Jambi province, in Sumatra, Indonesia. The considered lowlands in Jambi have a tropical humid climate, with annual mean temperature of 26.7 °C and annual mean precipitation of 2235 mm, with two main rainy peaks (March and December) and one dry season (July to August) (Drescher et al., 2016). The dominant soil type is a loamy Acrisol (Guillaume et al., 2015). The natural vegetation comprises tropical rainforest dominated by Dipterocarpaceae (Laumonier, 1997). Our study region originally covered with lowland rainforests was gradually transformed to agroforestry plantations and monocultures of oil palm (*Elaeis guineensis*), and rubber (*Hevea brasiliensis*) mainly (Clough et al., 2016).

2.2. The biodiversity enrichment experiment in oil palm EFForTS-BEE

The study was conducted in the Biodiversity Enrichment Experiment (EFForTS-BEE, https://treedivnet.ugent.be/ExpEFForTSBEE.html) that tests experimentally the suitability of mixed-species tree planting and natural regeneration to enhance biodiversity and ecosystem functions in existing oil palm plantations. The experiment was established in one oil palm plantation of PT. Humusindo Makmur Sejati (01.95° S and 103.25° E, 47 ± 11 m a.s.L) (Teuscher et al., 2016). Six tree species (*Parkia speciosa*, Fabaceae; *Archidendron pauciflorum*, Fabaceae; *Durio zibethinus*, Malvaceae; *Peronema canescens*, Lamiaceae; *Shorea leprosula*, Dipterocarpaceae; *Dyera polyphylla*, Apocynaceae) were selected based on their status as native to Sumatra and their importance for local communities (timber, latex, fruits). Around 40% of oil palms were felled prior to tree planting, with the number of felled oil palms depending on the plot size (for details see Gérard et al., 2017). In December 2013, after oil palm thinning, 6354 trees were planted on a 2-meter grid between the standing oil palms.

The experimental plots systematically varied in plot size and tree species diversity following a random partitions design (Teuscher et al., 2016). The experimental design was categorized into four partitions differentiated by the plot sizes (25 m^2, 100 m^2, 400 m^2, and 1600 m^2) (Fig. 1a), and further into blocks of different diversity levels (0, 1, 2, 3 or 6 tree species within each plot). A total of 52 experimental plots was established. No agrochemicals (neither mineral nor organic fertilizers) were applied in the experimental plots after tree planting, and manual weeding stopped after two years to allow natural regeneration (Teuscher et al., 2016). Four additional control plots measuring each 100 m^2 area, managed as-usual (i.e., application of organic and inorganic fertilizers, herbicides, occasional pesticides and manual weeding) and without planted trees were set. No tree species were planted in diversity-level-0 plots neither, but unlike control plots, diversity-level-0 plots were unmanaged (no herbicide, no fertilizers and no more weeding after two years to allow for natural regeneration). Three years after establishment of EFForTS-BEE, the experimental plots varied greatly in their structural complexity (Zemp et al., 2019a), canopy cover (Khokthong et al., 2019)

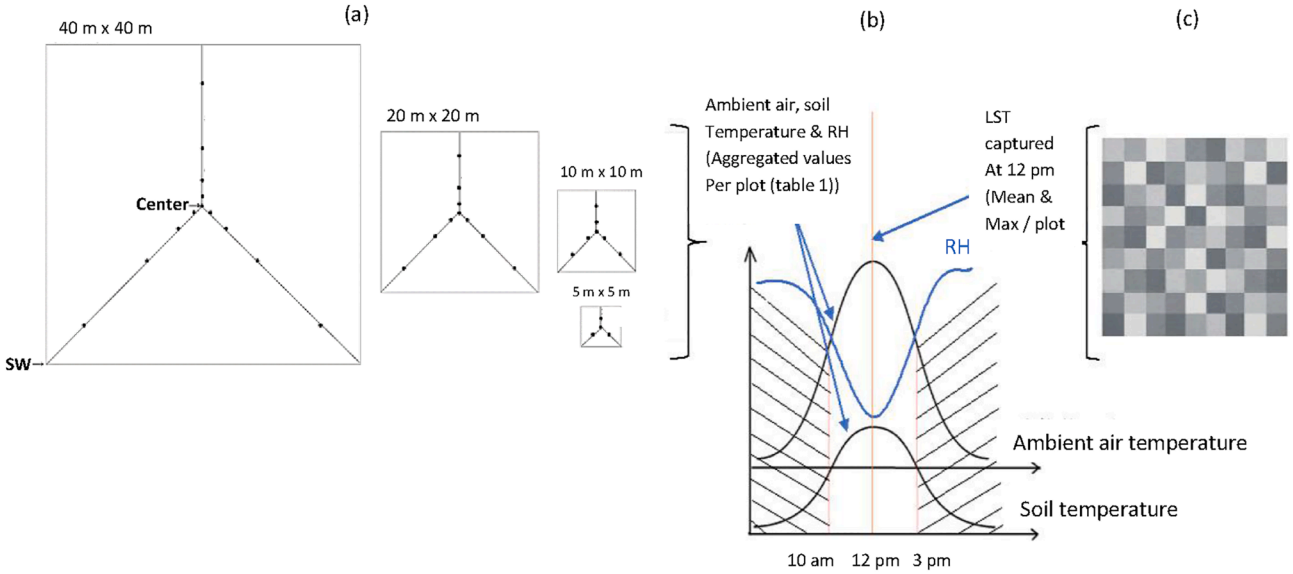

Fig. 1. General design for microclimate and LST data acquisition and analysis scheme. (a) Design for microclimate data acquisition for four different plot sizes. Each point represents one position of the mini microclimate sensors (a detailed representation with distances between mini microclimate sensors are represented in the Appendix (K); (b) Schematic representation of spatial and temporal frames considered for the analysis of microclimate and LST. Spatial variation is considered within plots and along elevational scale (soil, ambient air, canopy surface). Temporal scale is considered between 10 am and 3 pm for calculation of mean, median, max/min values and range of temperatures and relative humidity (Appendix B); (c) Thermal images of 0.113 m spatial resolution were acquired at noon for each plot.

and performance of the planted tree species (Zemp et al., 2019b). The productivity of the oil palms were affected by the experimental treatments and in particular by the thinning (Gérard et al., 2017).

2.3. Data acquisition

During the period 20th September 2017 to 26th September 2017, we acquired drone images and microclimate data (Appendix I). The installation of the mini microclimate sensors within the experimental plots and the daily flight missions were coordinated so that the data from both approaches could be directly compared.

2.3.1. Microclimate data

We deployed 198 miniaturized microclimate sensors (100 thermochron and 98 hygrochron iButtons, Maxim integrated, USA) to measure ambient air temperature, relative humidity, and soil temperature (Table 1), which were acquired in 10-minutes intervals all over considered days. Due to a limited number of available sensors, we selected from the 56 initial plots, 32 that represented a great variability in vegetation structure and with varying species diversity level and plot size, including the four control plots (Appendix C).

Within the plots, mini microclimate sensors were positioned on each sampling point located at increasing distance on a logarithmic scale (1, 2, 4 and 8 m distant from each other) oriented along three main directions: North, South-East, and South-West (Fig. 1a). The purpose of this fractal design was to account for spatial variations in temperature and humidity values (Hardwick et al., 2015) and to have comparable data across plot sizes (see also Section 2.4.2). We used two types of mini

Table 1
Meanings of important expressions used in data analyses.

Expressions	Explanation
Mean ambient air temperature	Average of all temperature values measured 1.5 m above the ground by mini microclimate sensors in a single plot (Appendix B) or from several plots (Appendix E & F) and in a precise time frame.
Median ambient air temperature	Middle value of distribution of all ambient air temperature values considered in a single plot (Appendix B) or from several plots (Appendix E & F) and in a precise time frame.
Standard error of mean ambient air temperature	Measure of dispersion of mean ambient air temperature values around the population mean in a single plot (Appendix B) or from several plots (Appendix E & F) and in a precise time frame.
Maximum ambient air temperature	Highest value of ambient air temperature measured in one or more plots and in a precise time frame.
Range of ambient air temperature	Difference between the highest and lowest ambient air temperature values in a single plot (Appendix B) or from several plots (Appendix E & F) and in a precise time frame.
Mean soil temperature	Average of all temperatures measured 10 cm under the ground by mini microclimate sensors in a single plot (Appendix B) or from several plots (Appendix E & F) and at a precise time.
Median, Standard error of mean, maximum, and range of soil temperature	Similar definitions applied for ambient air temperature, but considering soil temperature values.
Mean relative humidity (RH)	Average of all RH values measured 1.5 m above the ground by mini microclimate sensors in one or more plots and in a precise time frame.
Minimum RH	Lowest value of RH measured in a single plot (Appendix B) or from several plots (Appendix E & F) and in a precise time frame.
Median, Standard error of mean and range of RH	Similar definitions applied for ambient air and soil temperature, but considering RH values.
Mean land surface temperature (LST)	Average of all values of thermal pixels measured above the land surface in a single plot (Appendix B) or from several plots (Appendix E & F).
Median, Standard error of mean, maximum, and range of LST	Similar definitions applied for ambient air, soil temperature and RH, but considering LST values.
Species diversity level	Number of different tree species planted within a specific plot.
Stand structural complexity index	Vegetation structural complexity in a specific plot (Zemp et al., 2019a). Values were obtained from terrestrial laser scanning following the methodology described in Ehbrecht et al. (2017).

microclimate sensors: hygrochron temperature/humidity loggers (DS1923-F5#), installed 1.5 m above the ground to measure both the ambient air temperature and relative humidity and thermochron temperature loggers (DS1922L-F5#), placed 10 cm under the ground to measure soil temperature. The mini microclimate sensors were protected from water and direct solar radiations using hand-made multiplate radiation shields (Appendix L).

Precision and accuracy as provided by the manufacturer are 0.063 °C and 0.5 °C, respectively for hygrochron and thermochron loggers. When measured values were negative, these were considered as aberrant and therefore excluded from the analysis to prevent any bias. We corrected relative humidity values > 100% by adjusting them to 100%. We validated the mini microclimate sensors by applying a linear regression of the measured values with reference values (air temperature and relative humidity measured with Hygro-Thermo Transmitter, Thies Clima, Göttingen, Germany; soil temperature measured with Trime-Pico32, IMKO, Ettingen, Germany) across a range of controlled microclimatic conditions (25 °C - 35 °C), indicating no systematic biases (mean slope = 0.86, mean intercept = 5.68 °C, mean R^2 = 0.91 for temperature, mean slope = 0.96, mean intercept = 3.56%, mean R^2 = 0.91 for relative humidity) (Appendix G).

2.3.2. Drone images

We used thermal images acquired with an octocopter drone (MK EASY Okto V3; HiSystems, Moormerland, Germany) equipped with radiometric thermal and RGB cameras, to capture thermal and RGB images of all the 56 study plots. We used the thermal camera Flir Tau 2 640 with TeAx ThermoCapture module attached; the focal length 13 mm covers spectral bands ranging from 7.5 to 13.5 μm. RGB camera was based on an Omni vision OV12890 CMOS-Sensor 148 (Omni vision, USA) with a 170° FOV fish-eye lens (Ellsäßer et al., 2021). For each day considered, flights were operated at noon (12 pm local time) at the average height of 50 m above the starting point, but varying up to 20 m over plots. LST were determined from thermal pixels above correspondent surfaces.

2.3.3. Stand structural complexity

We derived the stand structural complexity from terrestrial laser scans in October and November 2016 (Zemp et al., 2019a), based on a procedure described by (Ehbrecht et al., 2021). A FARO Focus terrestrial laser scanner (Faro Technologies Inc., Lake Mary, USA), placed at the centre of each plot was used to obtain three-dimensional point clouds of each plot for the computation of the stand structural complexity index (SSCI). SSCI is an integrated measure of the three-dimensional arrangement of the vegetation above the herbaceous layer and quantifies the heterogeneity of biomass distribution in three-dimensional space (Ehbrecht et al., 2017). Index values increase with increasing efficiency of canopy space occupation and vertical stratification. Further details on SSCI construction and functioning can be found in Ehbrecht et al. (2021). Control plots considered to assess stand structural complexity, LST and microclimate were all different, and correlations between the three variable categories were therefore performed considering 28 plots instead of 32.

2.4. Statistical analyses

We used R version 3.6.3 to structure data and perform statistical analyses, and QGIS 3.2.3 to visualize thermal and RGB images and extract LST values for specific plots through image properties. For LST ramps determination, we changed properties of thermal images above plots of interest into single band pseudo-colour with linear interpolation. We calculated relevant metrics (mean, median, maximum/minimum, standard error of the mean and range) for ambient air temperature, relative humidity, soil temperature and LST. Relevant terminologies were used with their meanings summarized in Table 1.

2.4.1. Visualisation of temporal and spatial variability

We visualized the daily temporal variability of microclimate and the spatial variability of LST across plot size. To do so, we used data of a specific day (21st September 2017) showing the greatest extreme values of microclimate (Appendix I) from three plots (P50, P38 and P45 of respective sizes: 25 m^2, 400 m^2 and 1600 m^2). In the three plots, a total of 32 mini microclimate sensors was available (Appendix A) for data measurement. A visual assessment of RGB image's correlation to thermal images was performed. Additionally, Pearson's correlation coefficients were calculated for LST measured at noon and ambient air temperatures, considering the 28 plots with available data.

2.4.2. Influence of the number of mini microclimate sensors on microclimate estimates

By design, the number of mini microclimate sensors increased with plot size (Fig. 1a). We evaluated the influence of using an increasing number of mini microclimate sensors per plot on the microclimate variables. To do so, we selected the data from loggers at increasing distance from the plot centre and tested the effect of these subsets on the microclimate variables. We applied a linear mixed model using the *lme4* package (Bates et al., 2015), and the following formula: $y = \log(x + 1) + (1 + \log(x + 1) \mid Plot)$, with y being the microclimate variable (maximum ambient air temperature, minimum relative humidity, maximum soil temperature) in the corresponding subset and x the distance of the mini microclimate sensors from plot centre. The different plots can have varying slopes and intercepts, as introduced by the random effect. We evaluated the models using a type III Analysis of Variance (Appendix H) with Satterthwaite's method using the *lmerTest* package (Kuznetsova et al., 2017). Because we found an effect of the mini microclimate sensors number on max/min values (Appendix J), we considered the subset of four central mini microclimate sensors, one at plot centre and three 1 m away from plot centre (Fig. 1a), for all analyses concerning the effect of plot size on microclimate variables.

2.4.3. Effect of plot size, tree diversity level and structural complexity

Between 10 am and 3 pm local time, a time frame during which most of the spatial variability was expected, we calculated and compared mean and then maximum values per plot of ambient air temperature, soil temperature, and minimum RH between 4 size classes (25 m^2, 100 m^2, 400 m^2 and 1600 m^2) and control plots (100 m^2). The class of size 25 m^2 was excluded from analysis, as only one plot belonged to that category. We also compared mean and maximum values per plot of ambient air temperature, soil temperature, LST and minimum RH between 5 species diversity levels (0, 1, 2, 3, and 6) and control plots. Records on the 32 plots, including plot size and tree species diversity level were summarized in the Appendix D.

The effect of the experimental treatments (plot size and tree species diversity level) on microclimate variables was tested using an Analysis of Variance (ANOVA) followed by a Tukey's pairwise comparison test. Correlations between stand structural complexity index and microclimate variables were plotted and measured through Pearson's correlation.

3. Results

3.1. Temporal change of microclimate in experimental plots across plot sizes

The daily mean ambient air temperature and mean relative humidity (RH) followed similar patterns for each of the 7 days considered, with ambient air temperature peaks and RH minima around 3 pm. Soil temperature peaks were observed after 3 pm. Ambient air temperatures were higher than soil temperatures. The diurnal variation of the three variables was higher on 21st September 2017 than on the other recorded days (Appendix I). On that day, three plots of different sizes (25 m^2, 400 m^2 and 1600 m^2) showed similar diurnal patterns of ambient air

temperature, RH and soil temperature (Fig. 2). Therein, minimum ambient air temperature (28.9 °C) was reached at 6 am, followed by an increase from 8 am to a maximum of 38.7 °C at 3 pm; RH had high values until 8 am and a drop to a minimum of 48.2% at 3 pm. Within the timeframe 10 am – 3 pm, soil temperatures reached a maximum of 31.2 °C.

3.2. Correlation between ambient air temperature and LST

Both mean and maximum ambient air temperature were positively correlated with LST (Fig. 3). The correlations were strong and highly significant when considering maximum LST (r = 0.46–0.60; P = 0.01–0.001), intermediate for median LST (r = 0.37–0.41; P = 0.05–0.03) and relatively weak and only marginally significant when using minimum LST (r = 0.32–0.33, P = 0.10–0.09).

3.3. Land surface temperature variation within plots

Oil palm canopy cover influenced LST, with values as low as 28 °C observed above individual oil palms. High values of LST (37 °C and higher) were observed above bare soils and understorey vegetation. On the largest plot (Plot 45, 1600 m^2), a surprisingly warm zone was observed despite the presence of understorey tree species (Fig. 4). Generally, the range of observed LST increased with increasing plot size.

3.4. Microclimate in experimental plots versus in control plots

The microclimate in the experimental plots of varying sizes and diversity levels can be compared with the microclimate in the control plots (Fig. 5 and Fig. 6). Regarding experimental plots of varying sizes, mean values were in general not different than the control plots, except for plot size 100 m^2 that displayed higher mean air and soil temperature

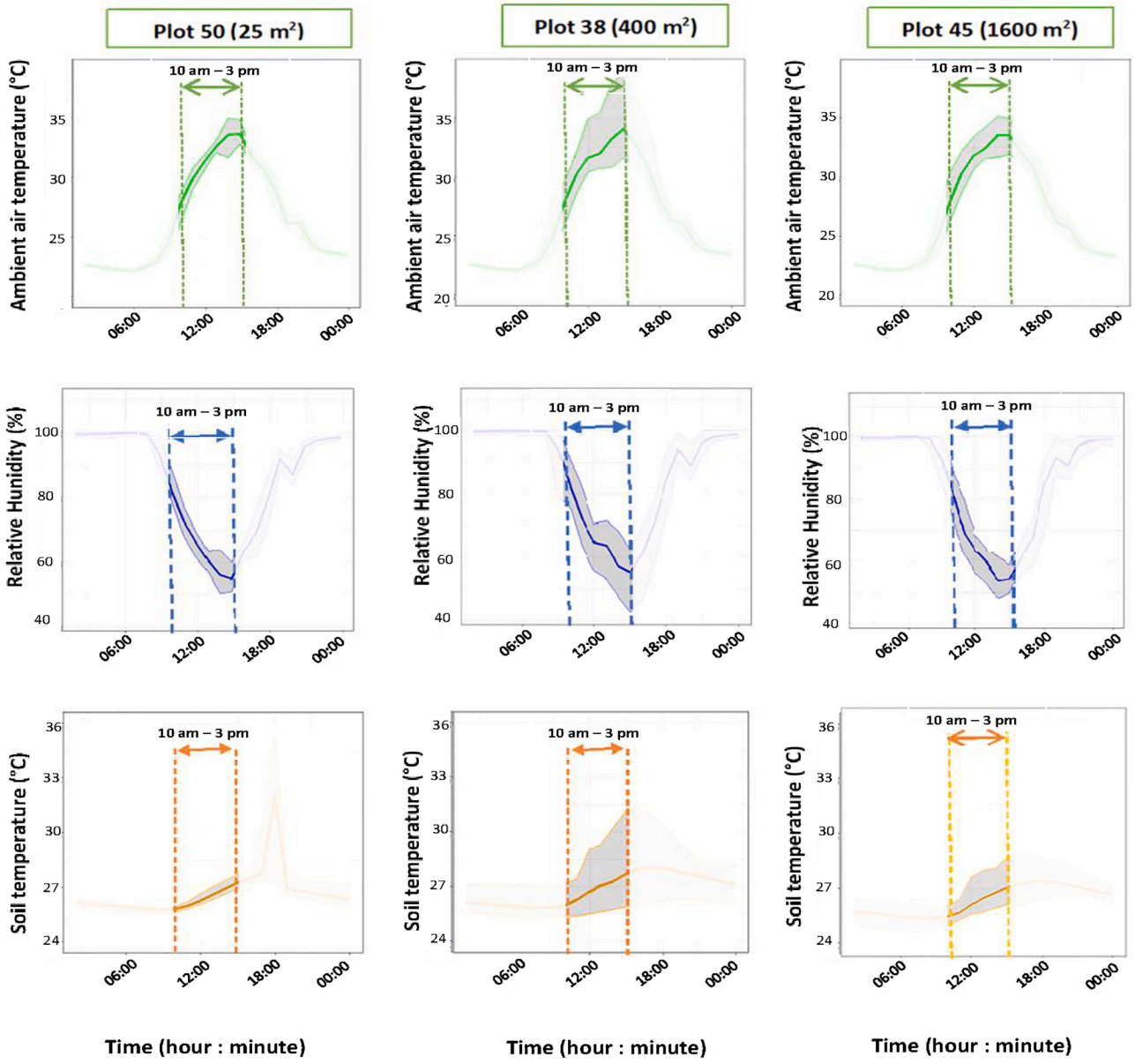

Fig. 2. Mean diurnal cycle of ambient air temperature (green), relative humidity (blue) and soil temperature (orange) expressed as hourly mean values and the range (grey shaded area) from 3 plots of sizes 25 m^2, 400 m^2 and 1600 m^2, and with respective diversity levels 6, 1 and 1. Temperature (ambient air and soil) and relative humidity, available at 10 min intervals, were aggregated as hourly values. Aggregation as hourly involved the determination of mean values of all microclimate values taken at 10 min intervals within each hour of the day. Only highlighted data within the timeframe 10 am to 3 pm local time were of interest. (For interpretation of the references to colour in this figure legend, the reader is referred to the web version of this article.)

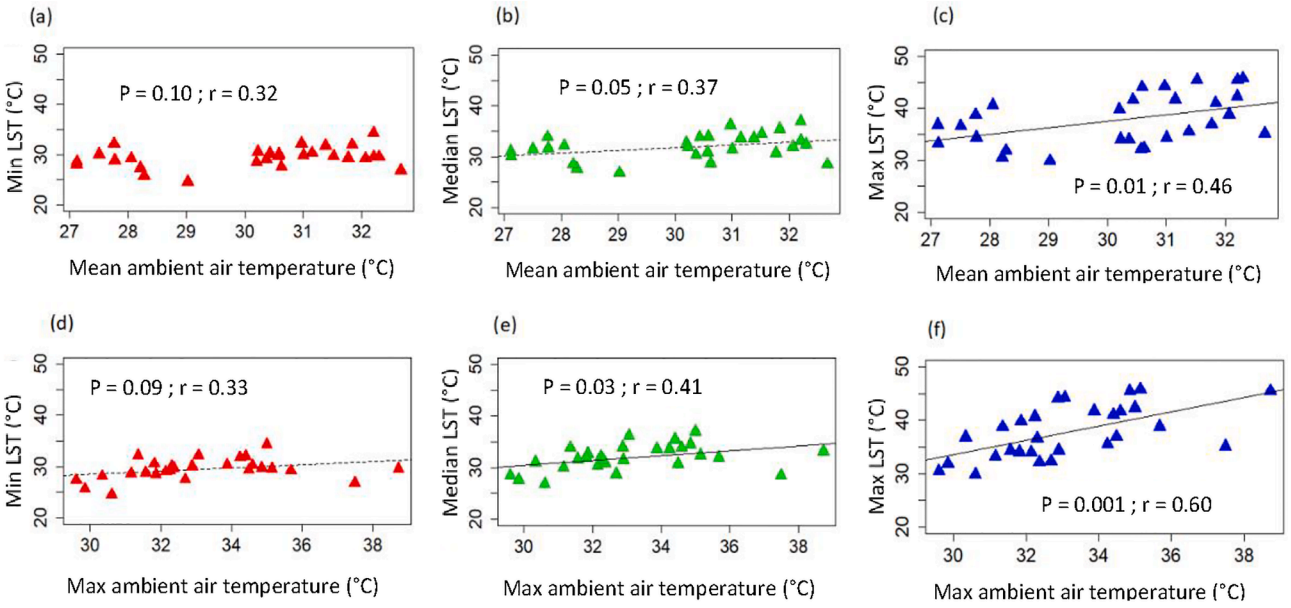

Fig. 3. Correlations between minimum (red; a & d), median (green; b & e) and maximum (blue; c & f) land surface temperatures (LST) and mean (upper row; a-c) and maximum (lower row; d-f) ambient air temperature values per plot. For the 28 plots in this study, LST were obtained from drone-recorded thermal images at 12 pm and ambient air temperature in the corresponding plots was measured with mini microclimate sensors (10 am – 3 pm local time). (For interpretation of the references to colour in this figure legend, the reader is referred to the web version of this article.)

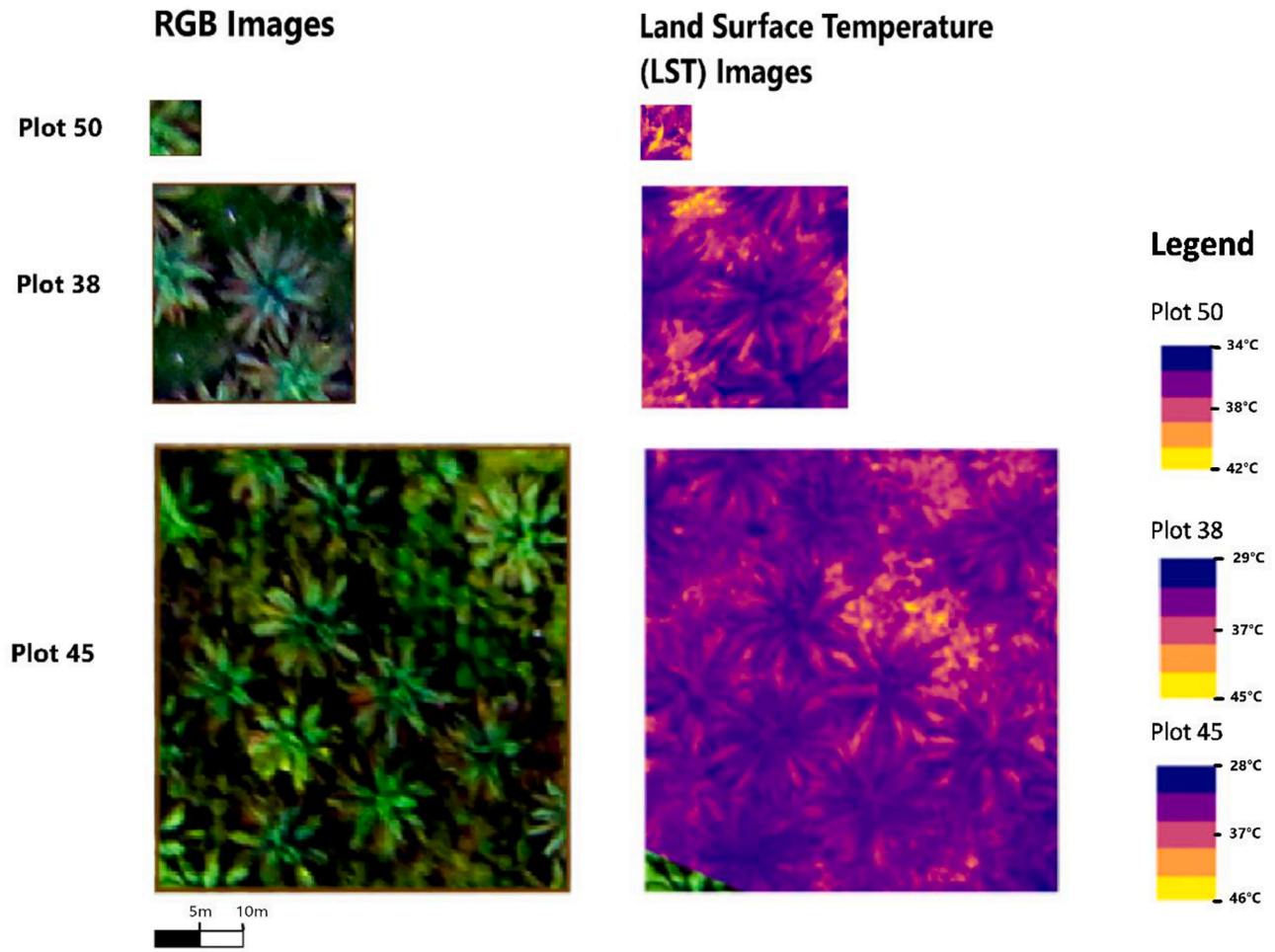

Fig. 4. Comparison between RGB images and LST images on three plots (P50, P38 and P45) of different sizes (25 m^2, 400 m^2 and 1600 m^2) and tree diversity levels (1 tree species planted in plots 38 and 45, and 6 tree species planted in plot 50). The same plots were used for the diurnal assessments in Fig. 2. The spatial resolution of the images was 0.113 m.

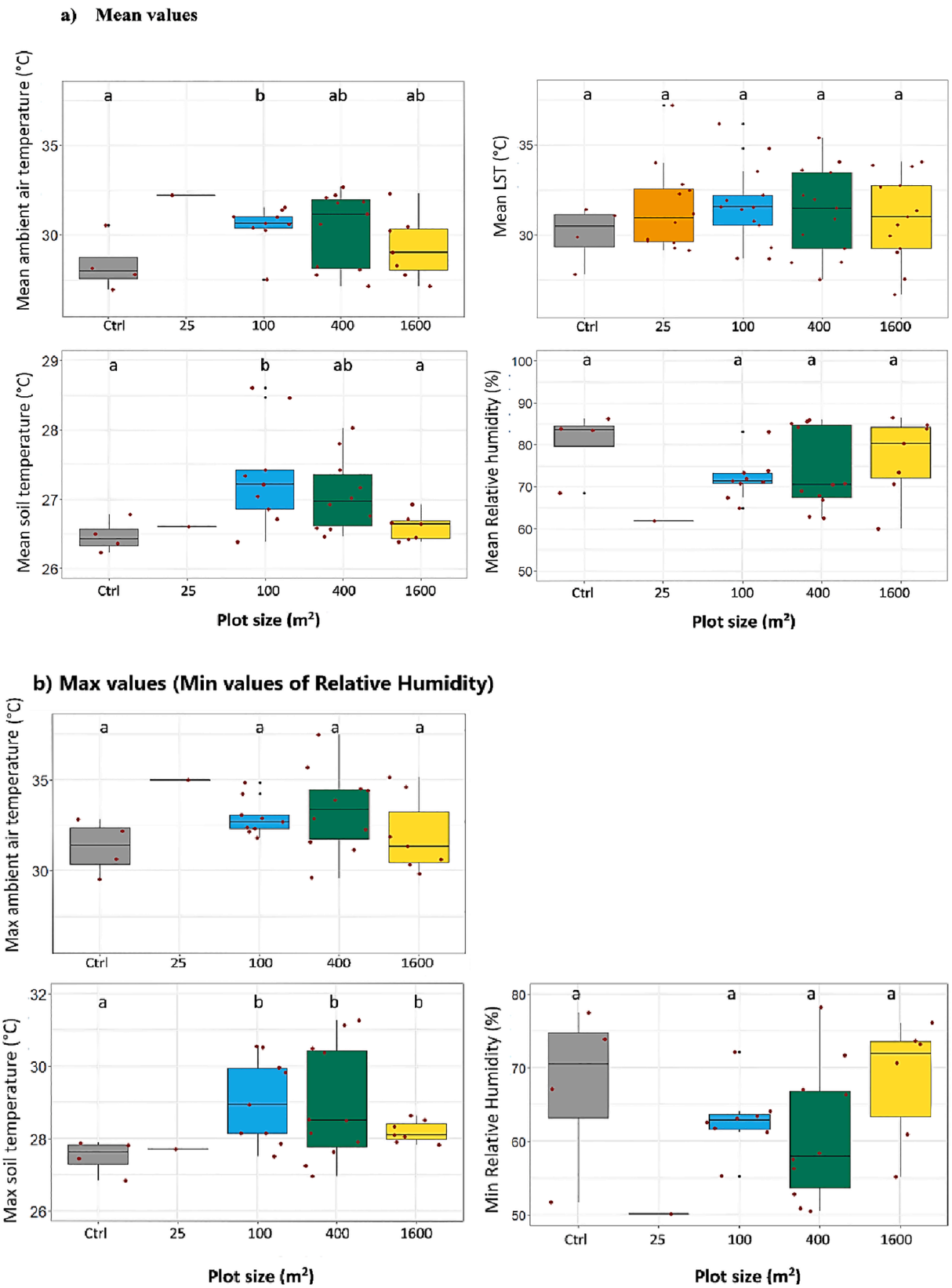

Fig. 5. Comparison of mean values per plot of ambient air temperature, relative humidity, soil temperature and LST (a) and maximum/minimum of the same variables per plot except LST (b), across different levels of plot size from 10 am to 3 pm local time. A subset of equal mini microclimate sensors number for all the plots was performed only for microclimate data (see Section 2.5.2), and not for thermal image pixels. The letters represent differences among mean/max/min microclimate and LST values of respective plot size classes (Tukey's pairwise test of independence).

than the control plot. Maximum soil temperatures within plot size categories 100 m^2, 400 m^2 and 1600 m^2 were higher than values within control plots. Experimental plots with planted trees (diversity level 1–6) showed some differences compared to the control plots, in particular for plots with diversity level 6 that had higher mean and max LST and max ambient air temperature, and plots with diversity level 1 that had higher mean soil temperature and max LST. Experimental plots where no trees were planted (diversity level 0) had higher mean and maximum ambient air temperature and LST and lower mean relative humidity, compared to the control plots.

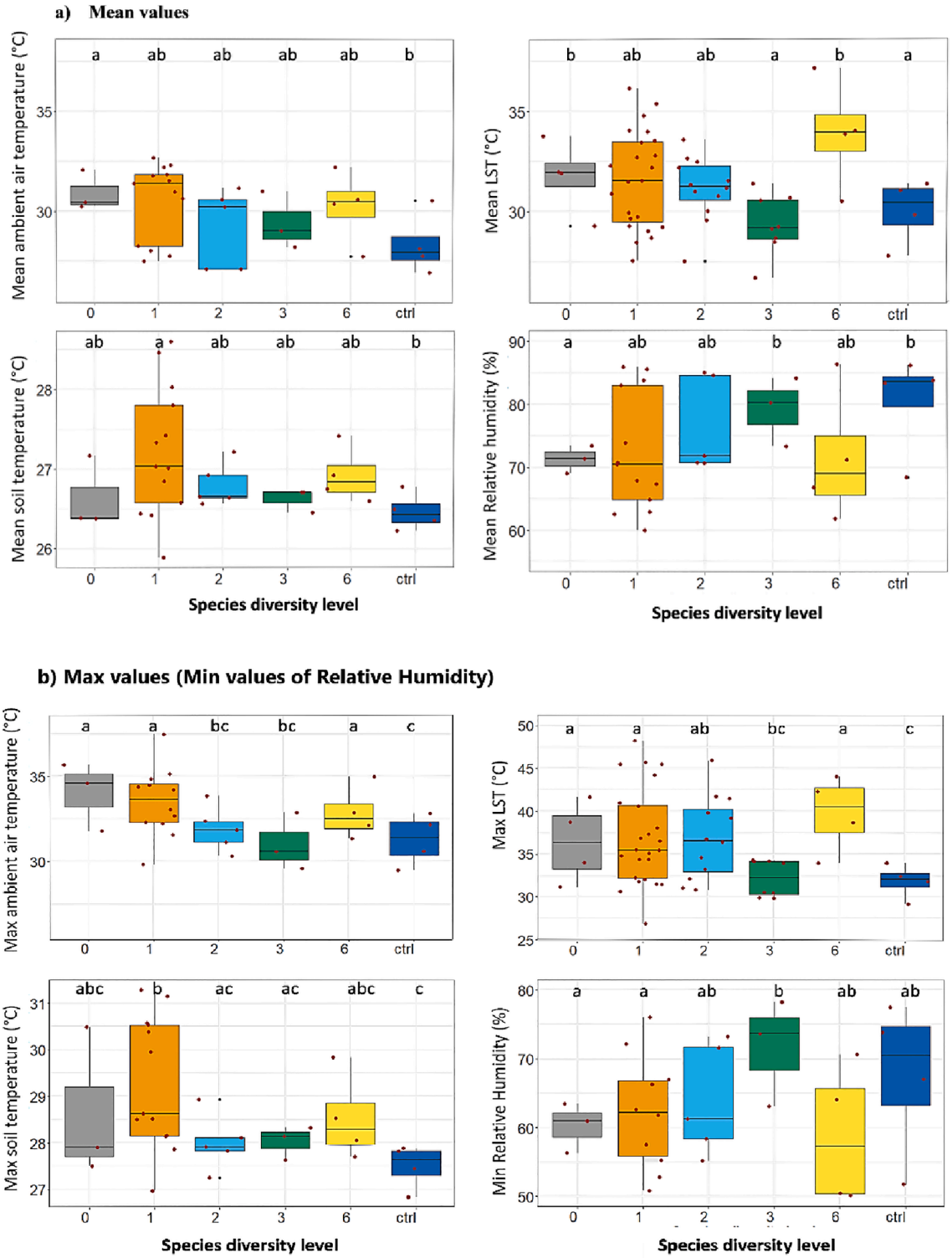

Fig. 6. Comparison of mean values per plot (a) and maximum/minimum values per plot (b) of ambient air temperature, relative humidity, soil temperature, and LST across different levels of species diversity (0, 1, 2, 3 and 6) from 10 am to 3 pm. The letters represent differences among mean/max/min values of respective diversity levels (Tukey's pairwise test of independence).

3.5. Effect of plot size on microclimate

Mean ambient air temperature ($F_{0.95} = 1.84$, $P = 0.15$), mean relative humidity ($F_{0.95} = 1.51$, $P = 0.23$), mean soil temperature ($F_{0.95} = 2.48$, $P = 0.07$), and mean LST ($F_{0.95} = 0.36$, $P = 0.83$) showed no significant differences across different plot sizes. Using maximum instead of mean values of the same variables yielded similar results. For mean ambient air and mean soil temperature, pairwise comparisons showed that control plots differed significantly from plots of size 100 m^2 (Fig. 5), but not from the other plot sizes.

In plots of 100 m^2, the highest values of mean ambient air temperature (30.56 ± 0.06 °C), soil temperature (27.46 ± 0.03 °C) and LST (31.63 ± 0.01 °C) were observed. Corresponding values were lower in the 1600 m^2 plots, respectively 29.56 ± 0.09 °C, 26.62 ± 0.02 °C and 30.96 ± 0.003 °C. In contrast, mean RH was highest in the 1600 m^2 plots, with 75.29 ± 0.46% (Appendix E). The range of ambient air temperature was highest in the size class 400 m^2, while LST had the highest range in the size class 1600 m^2. The observed ambient air temperature range was generally smaller than the LST range (Appendix E).

3.6. Effect of tree species diversity level on microclimate

The response to species diversity levels differed among the studied variables (Fig. 6). Mean ambient air temperature ($F_{0.95} = 1.34$, $P = 0.28$), mean relative humidity ($F_{0.95} = 1.004$, $P = 0.44$) and mean soil temperature ($F_{0.95} = 1.42$, $P = 0.25$) showed no significant differences, while mean LST ($F_{0.95} = 2.49$, $P = 0.04$) showed significant differences among diversity levels. Using maximum instead of mean values of the same variables yielded similar results. As for plot size, some pairwise comparisons showed significant differences (Fig. 6).

Mean ambient air temperature was highest within the diversity level 0, with 31.04 ± 0.05 °C, and lowest in plots of diversity level 3, with 29.17 ± 0.05 °C. Mean soil temperatures were highest in plots of diversity level 1 with 27.12 ± 0.02 °C, and lowest in diversity level 3 with 26.62 ± 0.02 °C. Mean LST were highest in diversity level 6, with 33.92 ± 0.013 °C, and lowest in diversity level 3, with 29.37 ± 0.006 °C. Mean RH showed the highest value (80.19 ± 0.22%) in diversity level 3 and the lowest (71.21 ± 0.20%) in diversity level 0 (Appendix F).

3.7. Effect of stand structural complexity on microclimate

The stand structural complexity influenced microclimate and LST across the 28 plots with available data. Mean and maximum values of ambient air temperature, soil temperature, and LST showed a negative correlation with SSCI while mean and minimum RH showed a positive correlation with SSCI (Fig. 7). Therein, the closest correlations were observed for mean and maximum ambient air temperature ($r = -0.49$ & $r = -0.55$ respectively).

4. Discussion

4.1. Spatial and temporal patterns of microclimate and LST

The daily microclimate variation over time followed a pattern characterised by highest ambient air temperatures and lowest RH values reached in the afternoon (3 pm). Meijide et al. (2018), while observing microclimate variables below the canopy in tropical agroforest systems (a jungle rubber), found that mean and range of ambient air temperatures reached their maxima in the early afternoon (2 pm). As Meijide et al. (2018) also confirmed, soil temperatures had unclear daily patterns with maximum values reached a bit later in the afternoon (around 6 pm).

Our initial hypothesis of a positive correlation between the ambient air and LST was met. The strongest correlations were observed between mean/maximum ambient air temperature and maximum LST. When comparing surface and ambient air temperature (at 1 m and 1.5 m height) in complex tropical rain forests, Scheffers et al. (2017) observed a significant positive and negative deviation from a slope of 1 when considering minimum and maximum LST, respectively. The authors also found that mean LST showed less deviation from the slope of 1, meaning a stronger correlation of mean LST with ambient air temperature in comparison to minimum and maximum LST. In contrast, for our study case, maximum LST showed higher correlations with mean and max ambient air temperature, compared to minimum and mean LST. The difference could be explained by the difference in the method of thermal data acquisition, with handheld cameras at 1 m height used by Scheffers et al. (2017), which reduced exposition level to solar radiations. Our increased footprint also offered a wider range of thermal observations with more extreme values (cooler oil palm canopies and hotter soil, stones, artefacts). It could also be justified by the size of plots considered which in our case was reduced. Hence, our and previous studies reflect the linkages between microclimate regulation and local canopy surface processes (Madigosky, 2004).

We observed a higher temperature range in LST compared to ambient air temperature, in agreement with previous studies (Scheffers et al., 2017), explained by increased aboveground habitat complexity and leaf density, thereby reducing the amount of incoming solar radiation reaching the ground surface. In fact, solar absorption by leaves and therefore decreased direct solar exposure of the soil reduces the light intensity conditioning the below-canopy microclimate (Gaudio et al., 2017). Additionally, the release of latent heat flux by the canopy via evapotranspiration has a cooling effect on the microclimate (Li et al., 2015), assuming very limited air turbulence below the canopy. Moreover, air humidity was higher below the canopy, consequently having higher heat capacity compared to the above-canopy dry air, which may further promote below- and above-canopy temperature differences. Moist air also absorbs more of the upwelling thermal radiation that might have interfered with the LST measurements.

LST distribution across the 3 specific plots (Fig. 4) depends on the vegetation type, with lower temperatures occurring above oil palm and higher temperatures above some understorey vegetation and bare soils. As lower temperatures reflect higher transpiration, these results are in adequacy with (Röll et al., 2019) who observed a higher transpiration in commercial oil palm plantations compared to smallholder oil palm plantations. This illustrates that vegetation type determines water use and hence LST.

4.2. Effect of plot size

We found a lower mean soil temperature in the plot size category 1600 m^2, compared to 100 m^2. This could be explained by edge effects, as the surrounding oil palm plantation will have greater effect on smaller plots (which have a higher edge-area fraction) (Mauya et al., 2015). Teuscher et al. (2016), showed additionally that large-sized tree islands positively influenced biodiversity and ecological functions, which in the present study can be justified by more favourable microclimate conditions. In fact, we found a tendency of faster air saturation in larger plots, compared to smaller plots (Fig. 5; Appendix J). This suggests that larger plots have a higher capacity to maintain a spatially homogeneous

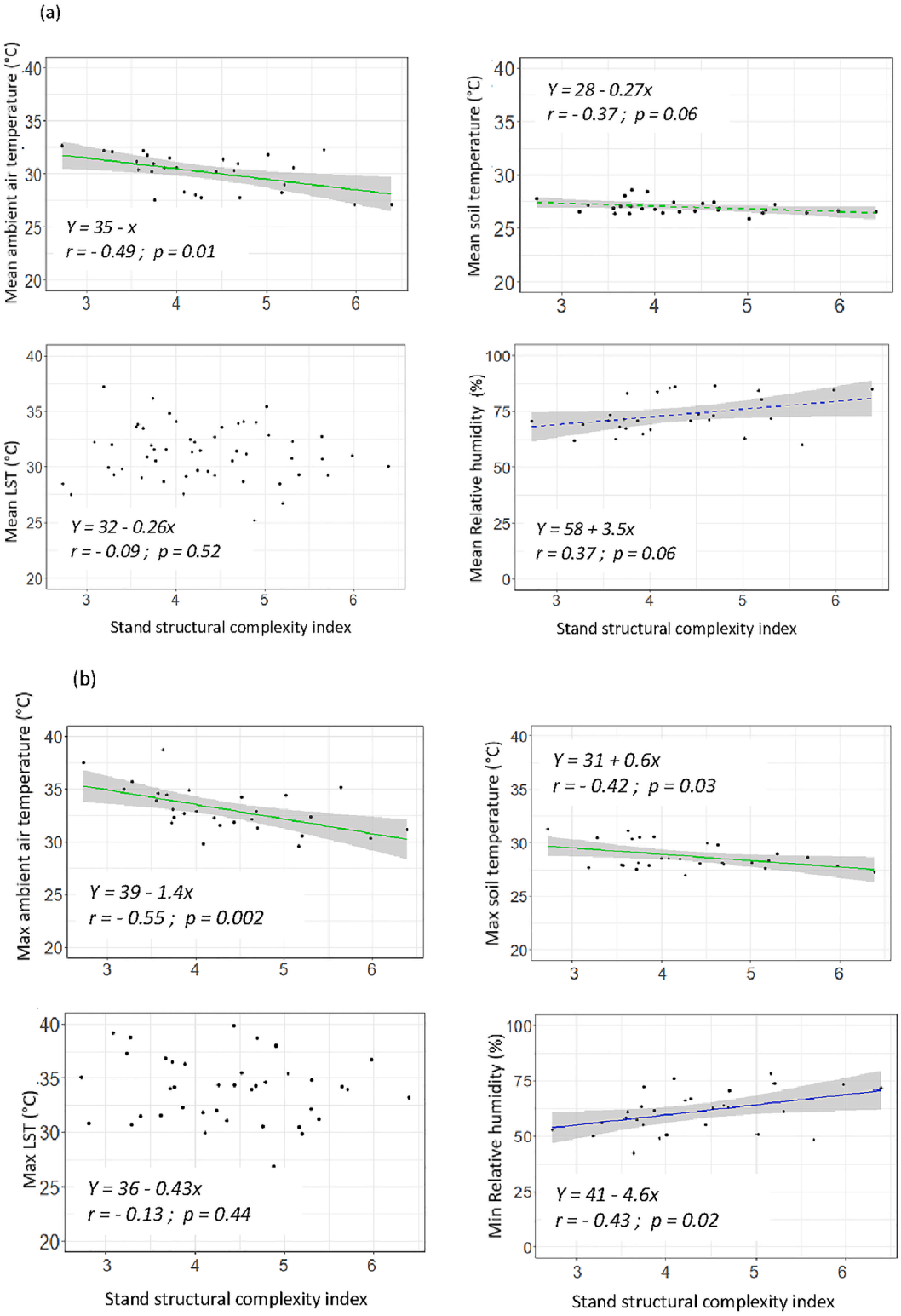

Fig. 7. Correlations of stand structural complexity index (SSCI) per plot with mean values per plot (a) and maximum/minimum values per plot (b) of ambient air temperature, relative humidity, soil temperature and LST. Full green and blue lines are represented where correlations are significant, dotted lines show less significant correlations, and no line is represented for weak correlations. Green lines correspond to trend lines related to temperatures and blue lines are related to relative humidity. The full range (grey shaded area) is represented for all cases. (For interpretation of the references to colour in this figure legend, the reader is referred to the web version of this article.)

Table A
State of mini microclimate sensor used for the study (with and without data).

Plot	Size	Position of sensors	Mini microclimate sensor id		
			With available data	Without data	Total available
Ctl1	100 m^2	Ambient air	23D, 23J, 23G, 23B, 23H, 23L, 23I, 23M	23E, 23F, 23C, 23K, 23A	8/13
		Soil	23Fs, 23Js, 23Cs, 23Ls, 23As, 23Is, 23Ms	23Es, 23Ds, 23Gs, 23Ks, 23Bs, 23Hs,	7/13
Ctl2	100 m^2	Ambient air	36, 12, 52, 9, 13, 20, 44, 22, 10, 35, 11	51, 17	11/13
		Soil	51s, 36s, 12s, 52s, 17s, 9s, 13s, 20s, 44s, 22s, 10s, 35s, 11s		13/13
Ctl3	100 m^2	Ambient air	12, 52, 9, 13, 44, 22, 10, 35	51, 36, 17, 20, 11	8/13
		Soil	36s, 12s, 17s, 20s, 22s, 10s, 11s	51s, 52s, 9s, 13s, 44s, 35s	7/13
Ctl4 (P53)	100 m^2	Ambient air	28, 34, 26, 27, 32, 29, 50C, 38	41, 6, 80B, 50A, 50D	8/13
		Soil	41s, 6s, 28s, 34s, 26s, 50As, 50Ds	27s, 32s, 80Bs, 29s, 50Cs, 38s	7/13
P50	25 m^2	Ambient air	50A, 50B, 50C	50D	3/4
		Soil	50As, 50Bs, 50Cs, 50Ds		4 /4
P9	100 m^2	Ambient air	45, 30, 53, 39, 54, 42	48	6/7
		Soil	45s, 48s, 30s, 53s, 39s, 42s	54s	6/7
P11	100 m^2	Ambient air	37, 1, 2, 5, 8, 3, 46		7/7
		Soil	37s, 1s, 2s, 5s, 8s, 3s, 46s		7/7
P13	100 m^2	Ambient air	21C, 21B, 21F, 21A, 21E, 21G	21D	6/7
		Soil	21Cs, 21Bs, 21Ds, 21Fs, 21As, 21Es	21gs	6/7
P14	100 m^2	Ambient air	14, 50B, 50C, 38, 50A, 29	50D	6/7
		Soil	14s, 50Bs, 50Cs, 38s, 50As, 50Ds	29s	6/7
P20	100 m^2	Ambient air	37, 1, 2, 5, 8, 3, 46		7/7
		Soil	37s, 1s, 2s, 5s, 8s, 3, 46s		7/7
P21	100 m^2	Ambient air	21C, 21B, 21F, 21A, 21E, 21G	21D	6/7
		Soil	21Cs, 21Bs, 21Ds, 21Fs, 21As, 21Es	21Gs	6/7
P27	100 m^2	Ambient air	37, 1, 2, 5, 8, 3, 46		7/7
		Soil	37s, 1s, 2s, 5s, 8s, 3s, 46s		7/7
P37	100 m^2	Ambient air	6, 28, 34, 26, 27, 32	41	6/7
		Soil	41s, 6s, 28s, 34s, 26s, 27s, 32s		7/7
P41	100 m^2	Ambient air	6, 28, 34, 26, 27, 32	41	6/7
		Soil	41s, 6s, 28s, 34s, 26s, 27s, 32s		7/7
P2	400 m^2	Ambient air	47, 18, 55, 43, 31, 24, 40, 33	15, 25	8/10
		Soil	47s, 15s, 55s, 43s, 24s, 33s, 25s	18s, 31s, 40s	7/10
P10	400 m^2	Ambient air	47, 18, 55, 43, 31, 24, 40, 33	15, 25	8/10
		Soil	47s, 15s, 55s, 43s, 24s, 33s, 25s	18s, 31s, 40s	7/10
P12	400 m^2	Ambient air	19D, 19H, 19F, 19I, 19A, 19G	19C, 19E, 19B, 19J	6/10
		Soil	19Es, 19Hs, 19Bs, 19Is, 19As, 19Gs	19Ds, 19Cs, 19Fs, 19Js	6/10
P15	400 m^2	Ambient air	6, 28, 34, 26, 27, 32, 50B, 50C	41, 80A	8/10
		Soil	41s, 6s, 28s, 34s, 26s, 50Bs, 50Cs	27s, 32s, 80As	7/10
P17	400 m^2	Ambient air	21C, 21B, 21F, 21E, 21G, 14, 7, 4	21D, 21A	8/10
		Soil	21Ds, 21Fs, 21As, 21Es, 14s, 7s, 4s	21Cs, 21Bs, 21Gs	7/10
P19	400 m^2	Ambient air	19D, 19H, 19F, 19I, 19A, 19G	19C, 19E, 19B, 19J	6/10
		Soil	19Es, 19Hs, 19Bs, 19Is, 19As, 19Gs	19Ds, 19Cs, 19Fs, 19Js	6/10
P30	400 m^2	Ambient air	37, 2, 5, 8, 3, 46, 38, 29	1, 50	8/10
		Soil	37s, 1s, 2s, 5s, 3s, 46s, 38s	8s, 50s, 29s	7/10
P36	400 m^2	Ambient air	47, 18, 55, 43, 31, 24, 40, 33, 25	15	9/10
		Soil	47s, 15s, 55s, 43s, 24s, 33s	18s, 31s, 40s, 25s	6/10
P38	400 m^2	Ambient air	19D, 19H, 19F, 10I, 19A, 19G	19C, 19B, 19J, 19E	6 /10
		Soil	19Es, 19Hs, 19Bs, 19Is, 19As, 19Gs	19Cs, 19Fs, 19Js, 19Ds	6 /10
P47	400 m^2	Ambient air	47, 15, 18, 55, 43, 31, 24, 40	25	8/9
		Soil	47s, 15s, 55s, 43s, 24s, 40s, 25s,	18s, 31s	7/9
P51	400 m^2	Ambient air	36, 12, 52, 9, 13, 44, 22	51, 17, 20	7/10
		Soil	51s, 36s, 12s, 17s, 9s, 20s, 22s	52s, 13s, 44s	7/10
P1	1600 m^2	Ambient air	23D, 23J, 23G, 23B, 23H, 23L, 23I, 23M	23E, 23F, 23C, 23K, 23A	8/13
		Soil	23Fs, 23Js, 23Cs, 23Ls, 23As, 23Is, 23Ms	23Es, 23Ds, 23Gs, 23Ks, 23bs, 23Hs	7/13
P7	1600 m^2	Ambient air	52, 9, 13, 44, 22, 10, 35	51, 36, 12, 17, 20, 11	7/13
		Soil	36s, 12s, 17s, 20s, 22s, 10s, 11s	51s, 52s, 9s, 13s, 44s, 35s	7/13
P23	1600 m^2	Ambient air	23D, 23J, 23G, 23B, 23H, 23L, 23I, 23M	23E, 23F, 23C, 23K, 23A	8/13
		Soil	23Fs, 23Js, 23Cs, 23Ls, 23As, 23Is, 23Ms	23Es, 23Ds, 23Gs, 23Ks, 23Bs, 23Hs	7/13
P24	1600 m^2	Ambient air	45, MA, ME, 30, MC, 53, MD, 42	MF, 54, MB, 39, 48	8/13
		Soil	MAs, MCs, MBs, 53s, MDs, 48s, 42s	45s, MEs, 30s, MFs, 54s, 39s	7/13
P35	1600 m^2	Ambient air	23D, 23J, 23G, 23B, 23H, 23L, 23I, 23M	23E, 23F, 23C, 23K, 23A	8/13
		Soil	23Fs, 23Js, 23Cs, 23Ls, 23As, 23Is, 23Ms	23Es, 23Ds, 23Gs, 23Ks, 23Bs, 23Hs	7/13
P45	1600 m^2	Ambient air	45, ME, 30, Mc, 53, MD, 42	48, MA, MF, 54, MB, 39	7 /13
		Soil	Mas, MBs, 53s, MDs, 48s, 42s	54s, 45s, Mes, 30s, MCs, MFs, 39s	6 /13
P46	1600 m^2	Ambient air	21F, 8, 21B, 3, 21E, 2, 21G, 5	46, 21D, 1, 21A	8/12 (D
		Soil	46s, 21Fs, 21Ds, 3s, 21As, 2s, 5s	8s, 21Bs, 1s, 21Es, 21Gs	7/12

Table B
Table of metrics of microclimate and LST variables per plot recorded between 10 am and 3 pm.

Plots N°	Max air t° (°C)	Mean air t° (°C)	Median air t° (°C)	Sd air t° (°C)	Min air t° (°C)	Max soil t° (°C)	Mean soil t° (°C)	Median soil t° (°C)	Sd soil t° (°C)	Max RH (%)	Mean RH (%)	Median RH (%)	Sd RH (%)	Min RH (%)	Max LST (°C)	Mean LST (°C)	Median LST (°C)	Sd LST (°C)	Min LST (°C)
1	29.8	28.3	28.6	1.1	25.2	28.5	26.4	0.6	26.3	100	83.8	82.7	4.6	76.1	31.8	27.6	27.6	0.8	25.6
2	29.6	28.2	28.6	1.0	25.3	27.6	26.5	0.5	26.4	100	84.2	82.8	4.2	78.3	30.5	28.5	28.5	0.5	27.3
7	30.6	29.0	29.4	1.1	25.8	28.3	26.7	0.9	26.8	100	80.3	79.3	4.2	73.7	29.8	26.7	26.7	0.7	24.5
9	32.9	31.0	31.1	1.0	28.8	28.2	26.7	0.6	26.7	100	73.3	72.6	5.5	63.1	34.3	31.4	31.4	0.6	29.9
10	35.7	32.1	32.0	1.5	29.1	30.5	27.2	0.8	27.0	100	69.1	68.5	6.3	56.3	38.8	32.0	31.9	1.0	29.2
11	34.2	31.4	31.4	1.3	28.7	30.0	27.3	0.9	27.1	100	73.8	73.6	5.9	62.7	35.5	33.5	33.6	0.7	31.7
12	37.5	32.7	32.4	2.0	29.7	31.3	27.8	1.1	27.6	100	70.5	70.9	7.7	52.8	35.1	28.5	28.4	0.9	26.8
13	34.9	31.5	32.2	1.9	27.7	30.6	28.5	1.1	28.6	100	64.9	61.4	11.0	49.0	45.5	34.8	34.5	2.5	29.7
14	32.7	30.6	30.9	1.0	28.1	27.9	26.9	0.6	27.0	100	70.8	70.7	4.7	61.8	32.2	28.7	28.7	0.5	27.5
15	32.2	28.0	27.0	2.1	25.7	28.5	27.4	0.5	27.5	100	85.6	90.4	9.1	66.4	40.6	32.2	32.1	1.6	29.2
17	34.5	31.8	31.8	1.2	29.3	30.4	28.0	0.9	27.9	100	67.9	67.5	5.4	57.5	36.9	30.9	30.7	1.0	29.3
19	32.9	30.6	31.2	1.6	27.6	28.5	26.8	0.5	26.7	100	66.9	62.9	10.9	50.5	44.1	34.1	33.9	1.6	30.0
20	33.1	31.0	31.3	1.5	28.0	28.2	27.0	0.5	27.0	100	67.4	64.8	9.3	55.3	44.2	36.2	36.2	1.5	32.2
21	32.1	30.4	30.6	0.9	28.1	29.8	27.4	1.0	27.3	100	71.2	71.5	3.9	64.1	34.0	30.5	30.3	0.9	29.0
23	31.3	27.8	26.9	1.9	25.9	28.1	26.9	0.4	26.9	100	86.4	91.1	7.9	70.7	38.7	33.9	33.8	0.8	32.1
24	31.9	30.2	30.8	1.4	27.4	28.1	26.6	0.5	26.6	100	70.7	67.1	10.2	55.2	39.8	32.7	32.6	1.7	28.4
27	32.4	30.6	30.7	0.9	28.4	28.9	27.2	0.8	27.1	100	71.9	72.3	4.1	61.3	32.1	30.8	30.8	0.4	29.6
30	31.6	27.8	27.1	1.8	25.7	27.0	26.6	0.2	26.6	100	86.0	90.7	8.3	67.0	34.3	31.5	31.6	0.9	28.8
35	34.6	30.4	30.3	1.1	28.4	27.9	26.4	0.5	26.3	100	73.5	74.2	4.6	61.0	41.6	33.8	33.8	1.4	30.2
36	33.9	31.2	31.1	1.1	29.0	27.9	26.9	0.5	27.0	100	70.7	71.3	4.7	58.4	41.7	33.6	33.6	1.4	30.3
37	31.8	30.2	30.3	0.8	28.2	27.5	26.4	0.6	26.3	100	71.4	71.4	4.0	63.5	34.0	31.9	31.9	0.6	30.5
38	38.7	32.2	32.0	1.9	29.1	31.1	27.0	1.1	26.8	100	62.5	63.1	7.5	42.5	45.5	33.4	33.1	2.4	29.5
41	32.3	27.5	28.2	2.2	23.7	30.5	28.6	0.7	28.5	100	83.0	80.2	7.3	72.2	36.5	31.5	31.4	0.9	30.1
45	35.1	32.3	32.4	1.4	29.2	28.6	26.4	0.7	26.2	100	60.0	59.2	6.7	48.2	45.7	32.7	32.3	1.9	29.5
46	30.3	27.1	28.0	2.0	23.4	27.8	26.7	0.5	26.6	100	84.6	82.5	6.5	73.2	36.8	31.0	31.0	1.2	28.0
47	31.2	27.1	27.9	2.0	23.5	27.3	26.6	0.4	26.5	100	85.1	82.9	6.8	71.7	33.2	30.0	30.0	0.7	28.6
50	35.0	32.2	32.4	1.6	28.9	27.7	26.6	0.5	26.6	100	61.9	61.2	7.2	50.2	42.3	37.2	37.0	1.5	34.2
51	34.4	31.8	31.8	1.4	28.9	28.2	25.9	2.4	26.5	100	63.0	62.3	6.5	50.9	41.0	35.4	35.4	1.5	31.9
ctl1	30.6	26.9	27.8	1.9	23.322	26.8	26.2	0.3	26.2	100	83.9	81.1	6.4	73.9	29.2	27.8	27.8	0.4	26.9
ctl2	32.2	27.8	26.9	1.9	25.691	27.5	26.4	0.3	26.3	100	86.2	90.6	8.3	67.1	31.8	29.9	29.9	0.7	28.4
ctl3	32.8	30.5	30.9	1.5	27.566	27.9	26.8	0.5	26.7	100	68.5	65.8	10.3	51.7	32.4	31.4	31.4	0.2	31.0
ctl4	29.5	28.1	28.4	1.0	25.5	27.8	26.5	0.6	26.5	100	83.4	82.0	4.0	77.5	34.0	31.1	31.0	0.8	29.3
															30.8	27.5	27.5	0.8	25.6
															30.6	29.3	29.3	0.4	28.0
															31.5	29.0	29.0	0.5	27.7
															26.9	25.2	25.1	0.6	24.0
															31.4	29.8	29.7	0.4	29.0
															29.9	29.1	29.1	0.2	28.6
															31.0	29.6	29.5	0.4	28.6
															34.6	31.2	31.2	1.1	28.8
															38.1	34.0	33.8	1.2	31.6
															45.9	31.3	31.1	1.8	27.9
															35.5	32.8	32.8	1.1	30.6
															34.1	30.6	30.5	0.7	28.9
															34.8	32.3	32.2	0.9	30.3
															39.2	32.2	31.8	1.6	29.6
															33.9	29.3	29.1	0.8	27.7
															36.4	31.6	31.4	0.9	30.3
															41.5	32.5	32.3	1.9	28.9
															31.2	29.3	29.2	0.5	28.4
															32.0	29.7	29.7	0.7	28.2
															37.3	30.0	29.9	0.8	28.0
															34.2	30.7	30.4	1.0	29.0
															30.5	28.7	28.7	0.5	27.7
															48.2	34.1	33.7	2.3	29.9
															34.4	29.3	29.2	0.7	27.7

Table C
State of plots with available mini microclimate sensors (hygrochron and thermochron) considering microclimate variables acquisition. Plot number with available and missing data, and percentage of available mini microclimate sensor were determined for each plot size category.

Plot sizes	25 m^2	Available mini microclimate sensor	100 m^2	Available mini microclimate sensor	400 m^2	Available mini microclimate sensor	1600 m^2	Available mini microclimate sensor	Control (100 m^2)	Available mini microclimate sensor
Plots and Available mini microclimate sensors	**P50**	Amb: 3/4	**P9**	Amb: 6/7	**P2**	Amb: 8/10	**P1**	Amb: 8/13	**Ctl1**	Amb: 8/13
		Soil: 4/4		Soil: 6/7		Soil: 7/10		Soil: 7/13		Soil: 7/13
			P11	Amb: 7/7	**P10**	Amb: 8/10	**P7**	Amb: 7/13	**Ctl2**	Amb: 11/13
				Soil: 7/7		Soil: 7/10		Soil: 7/13		Soil: 13/13
			P13	Amb: 6/7	**P12**	Amb: 6/10	**P23**	Amb: 8/13	**Ctl3**	Amb: 8/13
				Soil: 6/7		Soil: 6/10		Soil: 7/13		Soil: 7/13
			P14	Amb: 6/7	**P15**	Amb: 8/10	**P24**	Amb: 8/13	**Ctl4 (P53)**	Amb: 8/13
				Soil: 6/7		Soil: 7/10		Soil: 7/13		Soil: 7/13
			P20	Amb: 7/7	**P17**	Amb: 8/10	**P35**	Amb: 8/13		
				Soil: 7/7		Soil: 7/10		Soil: 7/13		
			P21	Amb: 6/7	**P19**	Amb: 6/10	**P45**	Amb: 7/13		
				Soil: 6/7		Soil: 6/10		Soil: 6/13		
			P27	Amb: 7/7	**P30**	Amb: 8/10	**P46**	Amb: 8/12		
				Soil: 7/7		Soil: 7/10		Soil: 7/12		
			P37	Amb: 6/7	**P36**	Amb: 9/10				
				Soil: 7/7		Soil: 6/10				
			P41	Amb: 6/7	**P38**	Amb: 6/10				
				Soil: 7/7		Soil: 6/10				
					P47	Amb: 8/9				
						Soil: 7/9				
					P51	Amb: 7/10				
						Soil: 7/10				
Sub-total plot / Available mini microclimate sensor (%)	**1 plot**	**84%**	**9 plots**	**87%**	**11 plots**	**71%**	**7 plots**	**57%**	**4 plots**	**66%**
Total plot Nb.	**32**									
Missing plot Nb.										

Table D
Plot sizes and diversity levels of planted tree species for investigated plots.

Plot ID	Plot sizes (m^2)	diversity level of planted tree species
50	25	6
9	100	3
11	100	1
13	100	1
14	100	1
20	100	1
21	100	6
27	100	2
37	100	0
41	100	1
53	100	ctrl
54	100	ctrl
55	100	ctrl
56	100	ctrl
2	400	3
10	400	0
12	400	1
15	400	1
17	400	1
19	400	6
30	400	1
36	400	2
38	400	1
47	400	2
51	400	1
1	1600	1
7	1600	3
23	1600	6
24	1600	2
35	1600	0
45	1600	1
46	1600	2

microclimate, and hence to regulate extreme microclimate values (Von Arx et al., 2013). According to Fonton et al. (2011), there should be a minimum reasonable plot size suitable to assess tree species behaviour. Most living organisms are microclimate dependent and, we were able to confirm that plot size regulates mean and extreme microclimate values over our study period.

4.3. Effect of species diversity and stand structural complexity

No significant effect of species diversity on microclimate nor on LST were observed, but few differences were observed between some categories (Fig. 6). For example, management-as-usual control plots had a lower max and mean LST and lower max ambient air temperature compared to the most diverse plots (diversity level 6). One reason to explain this is the fact that in the Biodiversity Enrichment Experiment, high transpiration by oil palms and relatively low transpiration by trees were observed (Ahongshangbam et al., 2019; Ellsäßer et al., 2021). The result also suggests that four years after establishment of the experiment, mixed-species tree planting does not yet enhance the buffering capacity of high temperatures in oil palm plantations, which is lower as compared to forests (Meijide et al., 2018). Recovery of ecosystem functions are long-term dynamics (Ghazoul and Chazdon, 2017) and further research is needed to investigate the effect of mixed-species tree planting on microclimate regulation over time.

We also found that plots with three species planted (diversity level 3) had a lower mean and max LST, higher mean and min RH and lower max air temperature, compared to plots where no trees were planted (diversity level 0). This could be explained by the performance of particular tree species (e.g., *Peronema canescens*, *Archidendron pauciflorum* and *Parkia speciosa*) and their complementarity in mixed neighbourhoods (Zemp et al., 2019b), which increased occupation of space and stand

Table E
Mean, median, standard error of mean, maximum/minimum values and ranges of microclimate variables (calculated considering individual mini microclimate sensor data) and LST (calculated considering individual pixel values) per plot size category (25 m^2, 100 m^2, 400 m^2 and 1600 m^2). Variables were determined within the time frame 10 am - 3 pm. Ambient air temperature, RH, and soil temperature variables were considered from 28 plots, whereas LST variables were considered from all 52 plots. The sample size for Se calculation was respectively the number of values measured by mini microclimate sensors for microclimate data, and the number of pixels for LST.

Plot size (m2) / (plot number)	Ambient air temperature (°C)					Soil temperature (°C)					Relative humidity (%)					Land Surface temperature (°C)				
	n = number of measurements by mini microclimate sensor; $n_{25} = 90$; $n_{100} = 930$; $n_{400} = 1050$; $n_{1600} = 630$															Total plot number = 52 / n = pixel number				
	Mean	Median	Se	Max	range	Mean	Median	Se	Max	range	Mean	Median	Se	Min	range	Mean	Median	Se	Max	range
25 / (1)	32.20	32.41	0.16	35.00	6.06	26.60	26.57	0.04	27.71	1.89	61.91	61.23	0.75	50.17	26.81	31.02	30.94	0.02	34.11	18.32
100 / (9)	30.56	30.74	0.06	34.24	10.55	27.46	27.28	0.03	28.83	5.04	71.69	71.77	0.26	50.08	49.92	31.63	31.53	0.01	35.78	18.00
400 / (11)	30.04	30.38	0.08	37.49	13.98	27.08	26.95	0.02	30.46	4.94	75.24	74.18	0.35	50.50	49.50	31.30	31.22	0.01	37.41	19.82
1600 / (7)	29.56	29.50	0.09	34.10	11.55	26.62	26.54	0.02	28.33	2.81	75.29	78.28	0.46	49.77	46.63	30.96	30.87	0.003	38.14	23.73

Appendix F

See Table F

Table F
Mean, median, standard error of mean, maximum/minimum values and ranges of microclimate variables (calculated considering individual mini microclimate sensor data) and LST (calculated considering individual pixel values) per category of tree species diversity (0, 1, 2, 3, and 6 tree species per plot). Variables were considered as described in the Appendix E.

Sp div level / (plot number)	Ambient air temperature (°C)					Soil temperature (°C)					Relative humidity (%)					Land urface temperature (°C)				
	n = number of values measured per plot by mini microclimate sensor $n_0 = 750$; $n_1 = 2940$; $n_2 = 1470$; $n_3 = 780$; $n_6 = 720$															Total plot number = 52 / n = pixel number				
	Mean	Median	Se	Max	range	Mean	Median	Se	Max	range	Mean	Median	Se	Min	range	Mean	Median	Se	Max	range
0 / (3)	31.04	30.82	0.05	35.68	7.56	26.64	26.53	0.02	30.50	5.12	71.21	71.54	0.20	56.30	29.54	31.74	31.70	0.006	36.40	13.25
1 / (13)	30.50	30.91	0.05	38.73	15.14	27.12	26.97	0.02	31.28	14.63	72.29	71.66	0.22	42.48	58.53	31.34	31.25	0.009	36.90	24.25
2 / (5)	29.19	29.68	0.06	33.87	10.51	26.77	26.69	0.02	28.94	3.38	76.64	76.35	0.26	55.21	46.86	31.16	31.07	0.009	36.92	20.27
3 / (3)	29.17	29.10	0.05	32.90	7.64	26.62	26.64	0.02	28.33	4.74	80.19	80.52	0.22	63.15	33.88	29.37	29.31	0.006	32.16	9.80
6 / (4)	29.67	30.06	0.08	35.00	9.23	26.94	26.85	0.02	29.84	4.01	74.67	73.46	0.46	50.17	45.93	33.92	33.73	0.013	39.76	15.07

Table M
Stand Structural Complexity indexes (SSCI) per plot.

Plot ID	SSCI
1	4.082572
2	5.165621
3	2.822266
4	3.301163
5	3.613564
6	4.879831
7	5.200806
8	3.393403
9	4.683438
10	3.281583
11	4.515193
12	2.73073
13	3.922131
14	3.865213
15	4.20872
16	4.112726
17	3.672592
18	4.359892
19	4.004061
20	3.74404
21	4.634974
22	4.788195
23	4.698118
24	4.435099
25	4.901599
26	4.183125
27	5.299723
28	5.042329
29	3.771563
30	4.270262
31	5.305847
32	3.081899
33	5.707363
34	3.88871
35	3.571496
36	3.552541
37	3.726377
38	3.631278
39	4.163249
40	5.380483
41	3.753486
42	4.242157
43	3.245299
44	5.646276
45	5.637914
46	5.976888
47	6.388292
48	4.756789
49	4.757572
50	3.188684
51	5.01727
52	4.43871

structural complexity (Zemp et al., 2019a). While natural regeneration provides multiple benefits (Ghazoul and Chazdon, 2017), our results indicate that mixed-species tree planting is more efficient for fast regulation of microclimate.

Lower temperatures and higher RH in more structurally complex plots expressed by the negative correlation between SSCI and mean/max ambient air temperature, and soil temperature (Fig. 7), confirmed our last hypothesis. One reason why experimental plots where no tree was planted (diversity level 0) had in general higher temperatures and lower humidity than the control plots in the conventional oil palm plantation is that, few years of natural regeneration did not yet lead to high structurally complexity (Zemp et al. 2019). These patterns might change over time as natural succession continues. However, it was more surprising that several experimental plots with planted trees exhibited higher air and soil temperature than control plots, despite the former being more structurally complex than the latter (Zemp et al. 2019a). One potential reason could be the thinning of oil palms that reduced canopy cover in the experimental plots (Khokthong et al., 2019). Here, most non-thinned (25 m^2 plots) plots were excluded from our analysis for practical reasons (there were not visible from drone images). Hence, maintaining canopy cover in the oil palm plantations and enhancing structural complexity appear appropriate for microclimate regulation. These results are in line with previous studies in other oil-palm dominated tropical landscapes, where canopy height clearly reduced extreme microclimate patterns (Jucker et al., 2018) and vegetation quality affected temperature and humidity (Williamson et al., 2020). Ehbrecht et al. (2019) observed that canopy cover is a major driver of microclimate and found a small effect of structural heterogeneity on diurnal thermal ranges in temperate forest ecosystems. Our results hence confirm the importance of vegetation and stand structural complexity to dampen microclimate and LST values. An efficient management of vegetation structural composition might consequently alleviate future extreme climatic patterns regarding the major problematic of climate change.

5. Conclusion

Combining microclimate and LST measured using mini microclimate sensors and drone-based thermal images respectively, our results revealed a positive correlation between the two variables. Overall, ambient air temperatures and LST were lower in mixed-species tree planting than in natural regeneration, but higher compared to conventionally managed oil palm plantations. In our experimental plots, we found that both larger plot sizes and stand structural complexity favour relatively low average temperatures, but high RH values. We conclude that an efficient management of structural variables in oil palm agroforestry might positively affect the microclimate or LST, and consequently positively contribute to biodiversity and ecosystem functions enhancement.

CRediT authorship contribution statement

Laura Donfack Somenguem: Conceptualization, Methodology, Data curation, Formal analysis, Writing - original draft. **Alexander Röll:** Writing - review & editing, Supervision. **Florian Ellsäßer:** Methodology, Investigation, Software, Writing - review & editing. **Martin Ehbrecht:** Methodology, Writing - review & editing. **Bambang Irawan:** Project administration, Methodology. **Dirk Hölscher:** Conceptualization, Funding acquisition, Methodology, Writing - review & editing. **Alexander Knohl:** Data curation, Writing - review & editing. **Holger Kreft:** Conceptualization, Funding acquisition, Methodology, Writing - review & editing. **Eduard J. Siahaan:** Methodology, Data curation. **Leti Sundawati:** Project administration, Methodology. **Christian Stiegler:** Methodology, Writing - review & editing. **Delphine Clara Zemp:** Conceptualization, Funding acquisition, Methodology, Investigation, Visualization, Writing - review & editing, Supervision.

Declaration of Competing Interest

The authors declare that they have no known competing financial interests or personal relationships that could have appeared to influence the work reported in this paper.

Table G1
Temperatures.

N°	Mini microclimate sensors' serial number	mini microclimate sensors' name	Count	Interception	P.Value	R^2	Slope	Standard error
1	640000004A8A0E41_temp	MFs	73	4.206	0	0.9409	0.873	0.0252
2	670000004A92D941_temp	23Hs	54	−0.367	0	0.9604	0.977	0.0277
3	670000004A92D941_temp	23Hs	55	14.61	0.0001	1	0.96	0.129
4	670000004A92D941_temp	23Hs	59	3.155	0	0.9216	0.859	0.0338
5	6A0000004A884541_temp	21Fs	54	7.32	0	0.9801	0.728	0.0133
6	6A0000004A884541_temp	21Fs	18	5.494	0	0.8649	0.769	0.075
7	6B0000004A8E9641_temp	N12s	73	4.383	0	0.9409	0.872	0.0251
8	6B0000004A8E9641_temp	N12s	54	7.714	0	0.9025	0.75	0.0325
9	6C0000004A8A4241_temp	40s	21	11.446	0	0.77	0.8	0.109
10	700000004A899B41_temp	2s	73	3.994	0	0.9409	0.885	0.0248
11	700000004A899B41_temp	2s	54	7.797	0	0.9025	0.742	0.0321
12	710000004A880741_temp	50Bs	31	15.603	0.0001	0.4096	0.527	0.1169
13	760000004A88B741_temp	MDs	16	4.154	0	0.9216	0.882	0.0708
14	790000004A7BD841_temp	N9s	52	3.295	0	0.9025	0.836	0.0402
15	7E0000004A845741_temp	19Es	54	2.123	0	0.9604	0.945	0.0253
16	7E0000004A845741_temp	19Es	21	11.494	0	0.77	0.8	0.1086
17	7E0000004A845741_temp	19Es	54	7.623	0	0.9216	0.756	0.0325
18	810000004A87C741_temp	23Bs	54	1.181	0	0.9604	0.973	0.0251
19	810000004A87C741_temp	23Bs	73	4.659	0	0.9409	0.866	0.0254
20	810000004A87C741_temp	23Bs	16	14.024	0	0.9025	0.52	0.0453
21	820000004A847A41_temp	51s	56	5.051	0	0.9216	0.8	0.0329
22	830000004E6A2941_temp	18	73	4.672	0	0.9409	0.867	0.0264
23	830000004E6A2941_temp	18	16	14.05	0	0.9025	0.516	0.0464
24	8B0000004A868141_temp	35s	73	4.07	0	0.9409	0.891	0.0253
25	960000004A930241_temp	N13s	73	0.99	0	0.9409	0.978	0.0266
26	960000004A930241_temp	N13s	18	5.469	0	0.8649	0.771	0.0746
27	980000004E685941_temp	19H	54	−5.888	0	0.9801	1.173	0.0258
28	980000004E685941_temp	19H	55	14.574	0.0001	1	0.95	0.1283
29	980000004E685941_temp	19H	59	2.987	0	0.9216	0.863	0.0322
30	9D0000004E69E341_temp	23I	54	5.879	0	0.9604	0.822	0.0255
31	9D0000004E69E341_temp	23I	60	2.075	0	0.9409	0.886	0.0285
32	A40000004A7D0F41_temp	16s	60	3.073	0	0.9409	0.848	0.0295
33	AD0000004E6A7941_temp	19	54	4.889	0	0.9604	0.855	0.0258
34	AD0000004E6A7941_temp	19	73	4.49	0	0.9409	0.872	0.0255
35	AE0000004A843941_temp	23Fs	54	0.727	0	0.9604	0.937	0.0253
36	AE0000004A843941_temp	23Fs	55	14.672	0.0001	1	0.96	0.1291
37	AE0000004A843941_temp	23Fs	18	5.346	0	0.8649	0.773	0.0737
38	AE0000004E664341_temp	14	73	4.713	0	0.9409	0.864	0.0264
39	AE0000004E664341_temp	14	54	8.142	0	0.9025	0.731	0.0327
40	B00000004A903541_temp	6s	21	11.337	0	0.77	0.81	0.1105
41	B00000004A903541_temp	6s	59	2.237	0	0.9216	0.875	0.0317
42	B10000004A866F41_temp	23Is	46	4.565	0	0.8281	0.811	0.0545
43	B10000004A866F41_temp	23Is	55	12.093	0	1	0.94	0.1177
44	B10000004A866F41_temp	23Is	60	3.349	0	0.9216	0.845	0.0329
45	B50000004E643341_temp	53	73	4.53	0	0.9409	0.873	0.0262
46	B50000004E671841_temp	21F	54	−7.911	0	0.9604	1.259	0.0336
47	B50000004E671841_temp	21F	22	7.534	0	0.62	0.9	0.1401
48	B50000004E671841_temp	21F	59	2.944	0	0.9216	0.863	0.0325
49	BA0000004A8B0041_temp	11s	34	2.734	0	0.8649	0.91	0.0643
50	BA0000004A8B0041_temp	11s	60	3.41	0	0.9216	0.841	0.0318
51	BD0000004E69CA41_temp	N6	46	−1.517	0	0.8464	1.048	0.0662
52	BD0000004E69CA41_temp	N6	73	4.341	0	0.9409	0.877	0.0255
53	BD0000004E69CA41_temp	N6	16	13.92	0	0.9025	0.519	0.0448
54	BF0000004A804041_temp	50As	21	11.421	0	0.77	0.8	0.1093
55	BF0000004A804041_temp	50As	58	3.247	0	0.9216	0.852	0.0341
56	C30000004A869F41_temp	53s	73	4.459	0	0.9409	0.876	0.025
57	C30000004A869F41_temp	53s	54	8.591	0	0.9025	0.724	0.0331
58	C70000004E686F41_temp	19A	46	−0.852	0	0.8836	1.031	0.0545
59	C70000004E686F41_temp	19A	73	4.504	0	0.9409	0.869	0.0255
60	C70000004E686F41_temp	19A	16	13.885	0	0.9025	0.521	0.0459
61	CD0000004E61E141_temp	19G	54	−6.531	0	0.9604	1.253	0.032
62	CD0000004E61E141_temp	19G	73	4.46	0	0.9409	0.871	0.0253
63	CE0000004A802641_temp	MAs	54	7.662	0	0.9216	0.756	0.0319
64	D40000004A8A1B41_temp	23Ls	46	9.666	0	0.7921	0.719	0.0563
65	D50000004E621E41_temp	21E	54	0.999	0	0.9604	0.977	0.0258
66	D50000004E621E41_temp	21E	73	4.33	0	0.9409	0.877	0.0253
67	D90000004A865841_temp	N15s	72	4.115	0	0.9409	0.887	0.0254
68	DB0000004A7D1041_temp	19Is	54	−2.988	0	0.9801	1.066	0.0253
69	DB0000004A7D1041_temp	19Is	55	14.234	0.0001	1	0.96	0.1294
70	DE0000004A896F41_temp	46s	60	3.433	0	0.9216	0.846	0.0339
71	E10000004A82C141_temp	41s	54	8.341	0	0.9025	0.728	0.0316
72	E40000004E69C941_temp	43	20	12.429	0	0.77	0.79	0.1127
73	E40000004E69C941_temp	43	54	7.553	0	0.9216	0.753	0.0307
74	E50000004A926E41_temp	19As	54	−1.882	0	0.9801	1.079	0.0253

(*continued on next page*)

Table G1 (*continued*)

N°	Mini microclimate sensors' serial number	mini microclimate sensors' name	Count	Interception	P.Value	R^2	Slope	Standard error
75	E50000004A926E41_temp	19As	73	4.566	0	0.9409	0.874	0.0252
76	E50000004A926E41_temp	19As	54	7.856	0	0.9025	0.748	0.0329
77	EC0000004A8DA941_temp	23As	54	8.463	0	0.9801	0.692	0.015
78	EC0000004A8DA941_temp	23As	21	10.6	0	0.77	0.79	0.1106
79	ED0000004A7D9441_temp	21As	46	0.915	0	0.8464	0.921	0.0577
80	ED0000004A7D9441_temp	21As	55	14.396	0.0001	1	0.97	0.1297
81	ED0000004A7D9441_temp	21As	18	5.07	0	0.8649	0.775	0.0753
82	EE0000004A8DBA41_temp	21Ds	54	−5.229	0	0.9801	1.134	0.0256
83	EE0000004A8DBA41_temp	21Ds	55	14.348	0.0001	1	0.97	0.1287
84	EE0000004A8DBA41_temp	21Ds	59	2.951	0	0.9216	0.861	0.033
85	F00000004A81F741_temp	42s	73	4.442	0	0.9409	0.873	0.025
86	F00000004A81F741_temp	42s	16	13.872	0	0.9025	0.525	0.0446
87	F70000004E675941_temp	21G	54	6.395	0	0.9604	0.759	0.0227
88	F70000004E675941_temp	21G	55	14.532	0.0001	1	0.96	0.1286
89	F70000004E675941_temp	21G	59	3.02	0	0.9216	0.864	0.0339
90	FA0000004E649D41_temp	47	73	4.742	0	0.9409	0.86	0.026
91	FC0000004E691D41_temp	N4	54	−1.091	0	0.9801	1.043	0.0245
92	FC0000004E691D41_temp	N4	73	4.454	0	0.9409	0.872	0.0254
Average values	5.683	0.000	0.913	0.856	0.050			

Table G2
Relative humidity.

N°	Mini microclimate sensors' serial number	mini microclimate sensors' name	Count	Interception	P.Value	R.2	Slope	Standard error
1	280000004E64E041_RH	50C	46	16.084	0	0.81	0.701	0.0516
2	530000004E696C41_RH	N5	54	−2.367	0	0.8649	0.991	0.0547
3	9D0000004E69E341_RH	23I	54	24.18	0	0.9409	0.553	0.0203
4	AD0000004E6A7941_RH	19	54	21.514	0	0.9025	0.594	0.0269
5	BD0000004E69CA41_RH	N6	46	15.152	0	0.7225	0.701	0.0646
6	C70000004E686F41_RH	19A	46	15.285	0	0.7921	0.706	0.0557
7	CD0000004E61E141_RH	19G	54	−19.883	0	0.8836	1.296	0.0627
8	D50000004E621E41_RH	21E	54	10.96	0	0.8836	0.798	0.04
9	FC0000004E691D41_RH	N4	54	8.982	0	0.8836	0.813	0.0419
10	080000004E6B4E41_RH	25	55	−1.99	0	0.9801	1.101	0.0262
11	1E0000004E632B41_RH	6	55	−6.506	0	0.9604	1.156	0.0305
12	280000004E64E041_RH	50C	55	1.997	0	0.9801	1.011	0.0197
13	430000004E667341_RH	N7	22	2.836	0.0001	0.5625	1	0.1959
14	530000004E696C41_RH	N5	55	0.843	0	0.9801	1.03	0.0201
15	830000004E6A2941_RH	18	55	−4.273	0	0.9604	1.123	0.0282
16	AD0000004E6A7941_RH	19	55	1.511	0	0.9801	1.022	0.0174
17	AE0000004E664341_RH	14	55	−2.893	0	0.9801	1.113	0.0239
18	B50000004E643341_RH	53	55	−5.97	0	0.9801	1.155	0.0259
19	BD0000004E69CA41_RH	N6	55	0.834	0	0.9801	1.025	0.0216
20	C70000004E686F41_RH	19A	55	2.42	0	0.9801	1.01	0.0188
21	CD0000004E61E141_RH	19G	55	0.576	0	0.9801	1.044	0.0211
22	D50000004E621E41_RH	21E	55	−1.016	0	0.9801	1.073	0.0217
Average				3.558	0.00	0.907636	0.955273	0.040427

Table H
Result of ANOVA test between distances from plot centre for three variables (maximum ambient air temperature, maximum soil temperature, minimum relative humidity). See corresponding illustrations in Appendix J.

Variables	Sum Sq	Mean Sq	NumDF	DenDF	F value	Pr(>F)
Max ambient air temperature	1.095	1.095	1	32.39	12.70	0.001162 **
Max soil temperature	4.84	4.84	1	25.04	37.30	2.189e-06 ***
Min relative humidity	15.57	15.57	1	31.58	19.57	0.0001077 ***

Acknowledgements

This research was funded by the Deutsche Forschungsgemeinschaft (DFG, German Research Foundation) – project number 192626868 – SFB 990 in the framework of the collaborative German – Indonesian research project CRC 990.

Access R script and useful data: donfacksomen / MIcroclimate and Land surface temperature _ data analysis script · GitLab (gwdg.de) or email Corresponding author.

References

Abood, S.A., Lee, J.S.H., Burivalova, Z., Garcia-Ulloa, J., Koh, L.P., 2015. Relative contributions of the logging, fiber, oil palm, and mining industries to forest loss in Indonesia. Conserv. Lett. 8 (1), 58–67. https://doi.org/10.1111/conl.2015.8.issue-110.1111/conl.12103.

Ahongshangbam, J., Khokthong, W., Ellsäßer, F., Hendrayanto, H., Hölscher, D., Röll, A., 2019. Drone-based photogrammetry-derived crown metrics for predicting tree and oil palm water use. Ecohydrology 12 (6), 163. https://doi.org/10.1002/eco.2115.

Banu, T.P., Borlea, G.F., Banu, C., 2016. The use of drones in forestry. J. Environ. Sci. Eng. B, 5(11). https://doi.org/10.17265/2162-5263/2016.11.007 M4 - Citavi.

Bates, D., Mächler, M., Bolker, B., Walker, S., 2015. Fitting linear mixed-effects models using lme4. J. Statist. Software 67(1). https://doi.org/10.18637/jss.v067.i01 M4 - Citavi.

Berni, J.A.J., Zarco-Tejada, P.J., Sepulcre-Cantó, G., Fereres, E., Villalobos, F., 2009. Mapping canopy conductance and CWSI in olive orchards using high resolution thermal remote sensing imagery. Remote Sens. Environ. 113 (11), 2380–2388. https://doi.org/10.1016/j.rse.2009.06.018 M4 - Citavi.

Böhnert, T., Wenzel, A., Altenhövel, C., Beeretz, L., Tjitrosoedirdjo, S.S., Meijide, A., Rembold, K., Kreft, H., 2016. Effects of land-use change on vascular epiphyte diversity in Sumatra (Indonesia). Biol. Conserv. 202, 20–29. https://doi.org/10.1016/j.biocon.2016.08.008.

Bonan, G.B., 2016. Ecological climatology (Third edit). Cambridge University Press.

Clough, Y., Krishna, V.V, Corre, M.D., Darras, K., Denmead, L.H., Meijide, A., Moser, S., Musshoff, O., Steinebach, S., Veldkamp, E., Allen, K., Barnes, A.D., Breidenbach, N., Brose, U., Buchori, D., Daniel, R., Finkeldey, R., Harahap, I., Hertel, D., Scheu, S., 2016. Land-use choices follow profitability at the expense of ecological functions in Indonesian smallholder landscapes. Nat. Commun. 7, 13137. https://doi.org/10.1038/ncomms13137 PM - 27725673.

De Frenne, P., Rodriguez-Sanchez, F., Coomes, D.A., Baeten, L., Verstraeten, G., Vellend, M., Bernhardt-Romermann, M., Brown, C.D., Brunet, J., Cornelis, J., Decocq, G.M., Dierschke, H., Eriksson, O., Gilliam, F.S., Hedl, R., Heinken, T., Hermy, M., Hommel, P., Jenkins, M.A., Kelly, D.L., Kirby, K.J., Mitchell, F.J.G., Naaf, T., Newman, M., Peterken, G., Petrik, P., Schultz, J., Sonnier, G., Van Calster, H., Waller, D.M., Walther, G.-R., White, P.S., Woods, K.D., Wulf, M., Graae, B.J., Verheyen, K., 2013. Microclimate moderates plant responses to macroclimate warming. PNAS 110 (46), 18561–18565. https://doi.org/10.1073/pnas.1311190110.

Drescher, J., Rembold, K., Allen, K., Beckschäfer, P., Buchori, D., Clough, Y., Faust, H., Fauzi, A. M., Gunawan, D., Hertel, D., Irawan, B., Jaya, I. N. S., Klarner, B., Kleinn, C., Knohl, A., Kotowska, M. M., Krashevska, V., Krishna, V., Leuschner, C., Scheu, S., 2016. Ecological and socio-economic functions across tropical land use systems after rainforest conversion. Philos. Trans. Roy. Soc. London. Series B, Biol. Sci. 371(1694). https://doi.org/10.1098/rstb.2015.0275 PM - 27114577.

Ehbrecht, M., Schall, P., Ammer, C., Seidel, D., 2017. Quantifying stand structural complexity and its relationship with forest management, tree species diversity and microclimate. Agric. For. Meteorol. 242, 1–9. https://doi.org/10.1016/j.agrformet.2017.04.012 M4 - Citavi.

Ehbrecht, M., Schall, P., Ammer, C., Fischer, M., Seidel, D., 2019. Effects of structural heterogeneity on the diurnal temperature range in temperate forest ecosystems. For. Ecol. Manage. 432, 860–867. https://doi.org/10.1016/j.foreco.2018.10.008 M4 - Citavi.

Ehbrecht, M., Seidel, D., Annighöfer, P., Kreft, H., Köhler, M., Clara Zemp, D., Puettmann, K., Nilus, R., Babweteera, F., Willim, K., Stiers, M., Soto, D., Juergen Boehmer, H., Fisichelli, N., Burnett, M., Juday, G., Stephens, S. L., Ammer, C., 2021. Global patterns and climatic controls of forest structural complexity. https://doi.org/10.1038/s41467-020-20767-z.

Ellsäßer, F., Stiegler, C., Röll, A., June, T., Hendrayanto, H., Knohl, A., Hölscher, D., 2021. Predicting evapotranspiration from drone-based thermography - a method comparison in a tropical oil palm plantation. https://doi.org/10.5194/bg-2021-159 M4 - Citavi.

FAO, 2017. Fao Food and Agricultural Policy Trend. 8, 2012–2017. http://www.fao.org/3/a-i7696e.pdf.

Faye, E., Rebaudo, F., Yánez-Cajo, D., Cauvy-Fraunié, S., Dangles, O., 2016. A toolbox for studying thermal heterogeneity across spatial scales: from unmanned aerial vehicle imagery to landscape metrics. Methods Ecol. Evol. 7 (4), 437–446. https://doi.org/10.1111/2041-210X.12488.

Fonton, N.H., Atindogbe, G., Hounkonnou, N.M., Dohou, R.O., 2011. Plot size for modelling the spatial structure of Sudanian woodland trees. Ann. Forest Sci. 68 (8), 1315–1321. https://doi.org/10.1007/s13595-011-0111-1 M4 - Citavi.

Foster, W.A., Snaddon, J.L., Turner, E.C., Fayle, T.M., Cockerill, T.D., Ellwood, M.D.F., Broad, G.R., Chung, A.Y.C., Eggleton, P., Khen, C.V., Yusah, K.M., 2011. Establishing the evidence base for maintaining biodiversity and ecosystem function in the oil palm landscapes of South East Asia. Philos. Trans. Roy. Soc. London. Series B, Biol. Sci. 366(1582), 3277–3291. https://doi.org/10.1098/rstb.2011.0041 PM - 22006968.

Gaudio, N., Gendre, X., Saudreau, M., Seigner, V., Balandier, P., 2017. Impact of tree canopy on thermal and radiative microclimates in a mixed temperate forest: A new statistical method to analyse hourly temporal dynamics. Agric. For. Meteorol. 237–238, 71–79. https://doi.org/10.1016/j.agrformet.2017.02.010.

Gérard, A., Wollni, M., Hölscher, D., Irawan, B., Sundawati, L., Teuscher, M., Kreft, H., 2017. Oil-palm yields in diversified plantations: Initial results from a biodiversity enrichment experiment in Sumatra, Indonesia. Agric., Ecosyst. Environ. 240, 253–260. https://doi.org/10.1016/j.agee.2017.02.026 M4 - Citavi.

Ghazoul, J., Chazdon, R., 2017. Degradation and recovery in changing forest landscapes: A multiscale conceptual framework. Annu. Rev. Environ. Resour. 42 (1), 161–188. https://doi.org/10.1146/annurev-environ-102016-060736.

Gibbs, H.K., Ruesch, A.S., Achard, F., Clayton, M.K., Holmgren, P., Ramankutty, N., Foley, J.A., 2010. Tropical forests were the primary sources of new agricultural land in the 1980s and 1990s. Proc. Natl. Acad. Sci. United States of America 107(38), 16732–16737. https://doi.org/10.1073/pnas.0910275107 PM - 20807750.

Guillaume, T., Damris, M., Kuzyakov, Y., 2015. Losses of soil carbon by converting tropical forest to plantations: erosion and decomposition estimated by δ(13) C. Glob. Change Biol. 21 (9), 3548–3560. https://doi.org/10.1111/gcb.2015.21.issue-910.1111/gcb.12907.

Hardwick, S.R., Toumi, R., Pfeifer, M., Turner, E.C., Nilus, R., Ewers, R.M., 2015. The relationship between leaf area index and microclimate in tropical forest and oil palm plantation: Forest disturbance drives changes in microclimate. Agric. For. Meteorol. 201, 187–195. https://doi.org/10.1016/j.agrformet.2014.11.010 PM - 28148995.

Hubbart, J., Link, T., Campbell, C., Cobos, D., 2005. Evaluation of a low-cost temperature measurement system for environmental applications. Hydrol. Process. 19 (7), 1517–1523. https://doi.org/10.1002/(ISSN)1099-108510.1002/hyp.v19:710.1002/hyp.5861.

IPBS, 2018. The IPBES assessment report on land degradation and restoration. In: Montanarella, L., Scholes, R., Brainich, A. (Eds.), Secretariat of the Intergovernmental Science-Policy Platform on Biodiversity and Ecosystem Services, Bonn, Germany, 744 pages.

Juchheim, J., Ehbrecht, M., Schall, P., Ammer, C., Seidel, D., 2019. Effect of tree species mixing on stand structural complexity. Forestry: Int. J. Forest Res. 111, 308. https://doi.org/10.1093/forestry/cpz046.

Jucker, T., Hardwick, S.R., Both, S., Elias, D.M.O., Ewers, R.M., Milodowski, D.T., Swinfield, T., Coomes, D.A., 2018. Canopy structure and topography jointly constrain the microclimate of human-modified tropical landscapes. Glob. Change Biol. 24 (11), 5243–5258. https://doi.org/10.1111/gcb.2018.24.issue-1110.1111/gcb.14415.

Kawashima, S., Ishida, T., Minomura, M., Miwa, T., 1999. Relations between Surface Temperature and Air Temperature on a Local Scale during Winter Nights.

Khokthong, W., Zemp, D.C., Irawan, B., Sundawati, L., Kreft, H., Hölscher, D., 2019. Drone-based assessment of canopy cover for analyzing tree mortality in an oil palm agroforest. Front. Forests Global Change 2, 259. https://doi.org/10.3389/ffgc.2019.00012 AR - 12 M4 - Citavi.

Koh, L.P., Levang, P., Ghazoul, J., 2009. Designer landscapes for sustainable biofuels. Trends Ecol. Evol. 24 (8), 431–438. https://doi.org/10.1016/j.tree.2009.03.012 PM - 19497636.

Kuznetsova, A., Brockhoff, P.B., Christensen, R.H.B., 2017. lmerTest Package: Tests in Linear Mixed Effects Models. J. Statistical Software 82(13). https://doi.org/10.18637/jss.v082.i13 M4 - Citavi.

Laliberte, A., 2009. Unmanned aerial vehicle-based remote sensing for rangeland assessment, monitoring, and management. J. Appl. Remote Sens. 3 (1), 33542. https://doi.org/10.1117/1.3216822 M4 - Citavi.

Laumonier, Y. (Ed.), 1997. The Vegetation and Physiography of Sumatra. Springer Netherlands, Dordrecht. https://doi.org/10.1007/978-94-009-0031-8 M4 - Citavi.

Li, Y., Zhao, M., Motesharrei, S., Mu, Q., Kalnay, E., Li, S., 2015. ARTICLE Local cooling and warming effects of forests based on satellite observations. Nat. Commun. 6 (1) https://doi.org/10.1038/ncomms7603.

Luskin, M.S., Potts, M.D., 2011. Microclimate and habitat heterogeneity through the oil palm lifecycle. Basic Appl. Ecol. 12 (6), 540–551. https://doi.org/10.1016/j.baae.2011.06.004 M4 - Citavi.

Madigosky, S.R., 2004. Tropical Microclimatic Considerations. In: Forest Canopies, Second Edition. Elsevier Inc., pp. 24–48. https://doi.org/10.1016/B978-012457553-0/50006-X

Mauya, E.W., Hansen, E.H., Gobakken, T., Bollandsås, O.M., Malimbwi, R.E., Næsset, E., 2015. Effects of field plot size on prediction accuracy of aboveground biomass in airborne laser scanning-assisted inventories in tropical rain forests of Tanzania. Carbon Balance Manage. 10, 10. https://doi.org/10.1186/s13021-015-0021-x PM - 25983857.

Meijaard, E., Brooks, T.M., Carlson, K.M., Slade, E.M., Garcia-Ulloa, J., Gaveau, D.L.A., Lee, J.S.H., Santika, T., Juffe-Bignoli, D., Struebig, M.J., Wich, S.A., Ancrenaz, M., Koh, L.P., Zamira, N., Abrams, J.F., Prins, H.H.T., Sendashonga, C.N., Murdiyarso, D., Furumo, P.R., Sheil, D., 2020. The environmental impacts of palm oil in context. Nat. Plants 1418–1426. https://doi.org/10.1038/s41477-020-00813-w). PM - 33299148.

Meijide, A., Badu, C.S., Moyano, F., Tiralla, N., Gunawan, D., Knohl, A., 2018. Impact of forest conversion to oil palm and rubber plantations on microclimate and the role of the 2015 ENSO event. Agric. For. Meteorol. 252, 208–219. https://doi.org/10.1016/j.agrformet.2018.01.013 M4 - Citavi.

Potter, K.A., Arthur Woods, H., Pincebourde, S., 2013. Microclimatic challenges in global change biology. Glob. Change Biol. 19 (10), 2932–2939. https://doi.org/10.1111/gcb.2013.19.issue-1010.1111/gcb.12257.

Qaim, M., Sibhatu, K.T., Siregar, H., Grass, I., 2020. Environmental, economic, and social consequences of the oil palm boom. Ann. Rev. Resource Econ. 12 (1), 321–344. https://doi.org/10.1146/annurev-resource-110119-024922.

Röll, A., Niu, F., Meijide, A., Ahongshangbam, J., Ehbrecht, M., Guillaume, T., Gunawan, D., Hardanto, A., Hendrayanto, Hertel, D., Kotowska, M.M., Kreft, H., Kuzyakov, Y., Leuschner, C., Nomura, M., Polle, A., Rembold, K., Sahner, J., Seidel, D., Zemp, D.C., Knohl, A., Hölscher, D., 2019. Transpiration on the rebound in lowland Sumatra. Agric. For. Meteorol. 274, 160–171. https://doi.org/10.1016/j.agrformet.2019.04.017.

Sabajo, C.R., Le Maire, G., June, T., Meijide, A., Roupsard, O., Knohl, A., 2017. Expansion of oil palm and other cash crops causes an increase of the land surface temperature in the Jambi province in Indonesia. Biogeosciences 14 (20), 4619–4635. https://doi.org/10.5194/bg-14-4619-2017 M4 - Citavi.

Scheffers, B.R., Edwards, D.P., Macdonald, S.L., Senior, R.A., Andriamahohatra, L.R., Roslan, N., Rogers, A.M., Haugaasen, T., Wright, P., Williams, S.E., 2017. Extreme thermal heterogeneity in structurally complex tropical rain forests. Biotropica 49 (1), 35–44. https://doi.org/10.1111/btp.2017.49.issue-110.1111/btp.12355.

Sequiño, A.C., Magallon-Avenido, J., 2015. The World's Leader in the Palm Oil Industry: Indonesia. IAMURE Int. J. Ecol. Conserv., 13(1). https://doi.org/10.7718/ijec.v13i1.1074 M4 - Citavi.

Shin, M., Patton, R., Mahar, T., Ireland, A., Swan, P., Chow, C.M., 2017. Calibration and validation processes for relative humidity measurement by a Hygrochron iButton. Physiol. Behav. 179, 208–212. https://doi.org/10.1016/j.physbeh.2017.06.019 PM - 28666935.

Teuscher, M., Gérard, A., Brose, U., Buchori, D., Clough, Y., Ehbrecht, M., Hölscher, D., Irawan, B., Sundawati, L., Wollni, M., Kreft, H., 2016. Experimental Biodiversity Enrichment in Oil-Palm-Dominated Landscapes in Indonesia. Front. Plant Sci. 7, 1538. https://doi.org/10.3389/fpls.2016.01538 PM - 27799935.

Vijay, V., Pimm, S.L., Jenkins, C.N., Smith, S.J., Anand, M., 2016. The impacts of oil palm on recent deforestation and biodiversity loss. PLoS ONE 11 (7), e0159668. https://doi.org/10.1371/journal.pone.0159668.

Von Arx, G., Graf Pannatier, E., Thimonier, A., Rebetez, M., 2013. Microclimate in forests with varying leaf area index and soil moisture: potential implications for seedling establishment in a changing climate. https://doi.org/10.1111/1365-2745.12121.

Williamson, J., Slade, E.M., Luke, S.H., Swinfield, T., Chung, A.Y.C., Coomes, D.A., Heroin, H., Jucker, T., Lewis, O.T., Vairappan, C.S., Rossiter, S.J., Struebig, M.J., Louzada, J., 2020. Riparian buffers act as microclimatic refugia in oil palm landscapes. J. Appl. Ecol. 58 (2), 431–442. https://doi.org/10.1111/jpe.v58.210.1111/1365-2664.13784.

Zellweger, F., Braunisch, V., Baltensweiler, A., Bollmann, K., 2013. Remotely sensed forest structural complexity predicts multi species occurrence at the landscape scale. For. Ecol. Manage. 307, 303–312. https://doi.org/10.1016/j.foreco.2013.07.023 M4 - Citavi.

Zellweger, F., Frenne, P., Lenoir, J., Rocchini, D., Coomes, D., 2019. Advances in microclimate ecology arising from remote sensing. Trends Ecol. Evol. 34 (4), 327–341. https://doi.org/10.1016/j.tree.2018.12.012 PM - 30651180.

Zellweger, F., Frenne, P., Lenoir, J., Vangansbeke, P., Verheyen, K., Bernhardt-Römermann, M., Baeten, L., Hédl, R., Berki, I., Brunet, J., van Calster, H., Chudomelová, M., Decocq, G., Dirnböck, T., Durak, T., Heinken, T., Jaroszewicz, B., Kopecký, M., Máliš, F., Coomes, D., 2020. Forest microclimate dynamics drive plant responses to warming. Science (New York, N.Y.), 368(6492), 772–775. https://doi.org/10.1126/science.aba6880 PM - 32409476.

Zemp, D.C., Ehbrecht, M., Seidel, D., Ammer, C., Craven, D., Erkelenz, J., Irawan, B., Sundawati, L., Hölscher, D., Kreft, H., 2019a. Mixed-species tree plantings enhance structural complexity in oil palm plantations. Agric. Ecosyst. Environ. 283, 106564. https://doi.org/10.1016/j.agee.2019.06.003.

Zemp, D.C., Gérard, A., Hölscher, D., Ammer, C., Irawan, B., Sundawati, L., Teuscher, M., Kreft, H., Isaac, M., 2019b. Tree performance in a biodiversity enrichment experiment in an oil palm landscape. J. Appl. Ecol. 56 (10), 2340–2352. https://doi.org/10.1111/jpe.v56.1010.1111/1365-2664.13460.